

Multi-period Mean Expected-Shortfall Strategies: "Cut your Losses and Ride Your Gains"

Peter A. Forsyth^a

Kenneth R. Vetzal^b

Sept. 19, 2022

Abstract

Dynamic mean-variance (MV) optimal strategies are inherently contrarian. Following periods of strong equity returns, there is a tendency to de-risk the portfolio by shifting into risk-free investments. On the other hand, if the portfolio still has some equity exposure, the weight on equities will increase following stretches of poor equity returns. This is essentially due to using variance as a risk measure, which penalizes both upside and downside deviations relative to a satiation point. As an alternative, we propose a dynamic trading strategy based on an expected wealth (EW), expected shortfall (ES) objective function. ES is defined as the mean of the worst β fraction of the outcomes, hence the EW-ES objective directly targets left tail risk. We use stochastic control methods to determine the optimal trading strategy. Our numerical method allows us to impose realistic constraints: no leverage, no shorting, infrequent rebalancing. For 5 year investment horizons, this strategy generates an annualized alpha of 180 bps compared to a 60:40 stock-bond constant weight policy. Bootstrap resampling with historical data shows that these results are robust to parametric model misspecification. The optimal EW-ES strategy is generally a momentum-type policy, in contrast to the contrarian MV optimal strategy.

Keywords: optimal control, expected shortfall, apparent alpha, tail risk, asset allocation, resampled backtests

JEL codes: G11, G22

AMS codes: 91G, 65N06, 65N12, 35Q93

1 Introduction

The Sharpe ratio is a commonly used measure of investment performance. However, the Sharpe ratio is easy to manipulate. Any strategy which includes non-linear payoffs (e.g. a portfolio including options) can produce an apparent outperformance (Dybvig and Ingersoll, 1982; Lhabitant, 2000; Goetzmann et al., 2002). As noted by Spurgon (2001), selling off the right side of the terminal wealth distribution can improve the Sharpe ratio. Such a strategy is simple to implement by owning the underlying asset and selling out of the money calls on the asset (covered call writing).

Of course, in a complete market options can be replicated by dynamically trading stocks and bonds. Consequently any portfolio containing options is equivalent to a dynamic trading strategy. Hence, Sharpe ratios can be maximized by using optimal stochastic control techniques, coupled with

^aDavid R. Cheriton School of Computer Science, University of Waterloo, Waterloo ON, Canada N2L 3G1, paforsyt@uwaterloo.ca, +1 519 888 4567 ext. 44415.

^bSchool of Accounting and Finance, University of Waterloo, Waterloo ON, Canada N2L 3G1, kvetzal@uwaterloo.ca, +1 519 888 4567 ext. 46518.

30 a suitable objective function. An interesting corollary to this observation is the use of stochastic
31 control in fraud detection (Bernard and Vanduffel, 2014).

32 Except for extremely pathological cases, a strategy which maximizes a mean-variance objective
33 function will also maximize the Sharpe ratio. In the dynamic trading context, a mean-variance
34 optimal strategy can be determined by minimizing a quadratic target objective function (Li and
35 Ng, 2000; Zhou and Li, 2000; Vigna, 2014). In a complete market, the optimal strategy never
36 exceeds the target (Cui et al., 2012; Vigna, 2014; Bauerle and Grether, 2015; Dang and Forsyth,
37 2016). Consequently, even though the risk measure is symmetric (i.e. the variance), the optimal
38 strategy produces a highly skewed terminal wealth distribution (Goetzmann et al., 2002; van Staden
39 et al., 2021).

40 A dynamic investment strategy which maximizes the Sharpe ratio also produces an *apparent*
41 alpha (Goetzmann et al., 2002) relative to a fixed proportion strategy. However, due to the highly
42 skewed distributions produced by these strategies, it is not clear that the resulting wealth distri-
43 bution is actually desired by the investor, in spite of these apparently good performance metrics.
44 Of course, it could be argued that variance is a poor risk measure in any case. Investors are more
45 concerned with downside risk measures. Indeed, upside volatility can be considered desirable.

46 As a result, in this paper, we propose using expected shortfall (ES) as the risk measure. ES is
47 simply the average of the worst β fraction of outcomes, and hence is a downside tail risk measure. ES
48 is basically the negative of the conditional value at risk (CVAR). Using stochastic control techniques,
49 we determine the optimal investment strategies which are Pareto optimal, with reward given by
50 expected terminal wealth (EW), and risk measured by ES. For medium-term investments (i.e. 2-5
51 years) the optimal EW-ES strategy generates a significant annualized alpha compared to constant
52 weight policies. The optimal controls are determined using a parametric model of stock and bond
53 processes, calibrated to 93 years of historical data. We verify that these strategies are robust to
54 parametric model uncertainty, by testing the strategies on bootstrapped resampled historical data.

55 It is interesting to observe that the Sharpe ratio maximizing dynamic strategy (or equivalently
56 quadratic shortfall minimizing) is fundamentally contrarian. Under this policy, when stocks increase
57 in value, they are sold, and assets shifted to bonds. When stocks decrease in value, stocks are bought,
58 and bond holdings reduced. However, we see the completely opposite policy in Pareto optimal EW-
59 ES strategies. The optimal EW-ES policy has more of a momentum character: when stocks go
60 up in value, stock holdings are increased. When stocks go down in value, stocks are sold, and
61 assets shifted to bonds. This is simply a consequence of the ES penalty; when the investor's wealth
62 is reduced, increasing the bond fraction protects against further moves to the downside. In fact,
63 this strategy provides a mathematical rationale for the trader's maxim "*Cut your losses, ride your*
64 *gains*".

65 Since the Sharpe ratio maximizing and EW-ES optimal strategies have fundamentally different
66 investment policies, and hence different terminal wealth distributions, each approach may appeal
67 to different investors, at different stages in their investment lifecycles. However, for medium-term
68 investors having wealth-preservation as a high priority, EW-ES strategies are worth considering.

69 We note that both the EW-ES and Sharpe ratio maximizing strategies are pre-commitment
70 polices, which are not formally time consistent. However, this is really just a matter of interpretation,
71 since for both strategies there is an equivalent induced objective function which generates the
72 same controls, yet is time consistent (Strub et al., 2019). Hence, in both cases, these policies are
73 implementable (Forsyth, 2020a). In addition, as noted by Bernard and Vanduffel (2014), if the EW-
74 ES strategy is realized in an investment product sold to a retail investor then the optimal policy
75 from the investor's point of view is in fact of pre-commitment type, since the retail client does not
76 herself trade in the underlying assets during the lifetime of the contract.

77 In the case of an investment product sold to a retail investor, we can envision that the investor

78 repeatedly buys the product for 2 – 5 year terms. Our results show that over a 5-year term, this
 79 product generates an alpha of 180 bps per year compared to a 60:40 stock-bond portfolio. Even for a
 80 2-year investment horizon, the EW-ES strategy generates an alpha of 120 bps per year compared to
 81 a 60:40 stock-bond portfolio. This product would be appealing to investors who want to outperform
 82 a typical constant weight strategy, but who are also concerned with worst case tail risk over 2 – 5
 83 year periods.

84 To begin, in Section 2, we review the known results for Sharpe ratio maximizing strategies,
 85 and define the alpha of these strategies relative to fixed weight policies. We also provide some
 86 illustrative results, documenting the performance of these strategies. We subsequently proceed to
 87 formally define the EW-ES problem, describe our algorithm for determination of the optimal control,
 88 define the appropriate alpha, and discuss the numerical results.

89 2 Background: Maximizing Sharpe Ratios and Defining Alpha

90 Let r be the risk-free return, and T be the investment horizon. W_t is the wealth of a portfolio at
 91 time t . The continuously compounded Sharpe ratio is then defined as

$$\mathbb{S} = \frac{E[W_T] - W_0 e^{rT}}{\text{std}[W_T]}, \quad (2.1)$$

92 where $E[\cdot]$ and $\text{std}[\cdot]$ respectively denote expectation and standard deviation. Note that \mathbb{S} is defined
 93 in terms of the terminal wealth and standard deviation at time T (Lhabitant, 2000; Goetzmann
 94 et al., 2002; Bernard and Vanduffel, 2014), in contrast to the *instantaneous* Sharpe ratio, which is
 95 defined in terms of averaging short period returns. Dynamic trading strategies will have different
 96 equity exposure over different short-term periods, and so averaging short period returns is not a
 97 meaningful metric.

Consider a market containing a stock index and a risk-free bond. Let the amount invested in
 the stock index be S_t , and the amount in the risk-free bond be B_t . We assume that

$$\begin{aligned} \frac{dS_t}{S_t} &= \mu dt + \sigma dZ \\ \frac{dB_t}{B_t} &= r dt, \end{aligned} \quad (2.2)$$

where μ is the stock drift rate, σ is the volatility, and dZ is the increment of a Wiener process. Let
 p be the fraction of the total portfolio W_t invested in the stock. Assuming continuous rebalancing,
 then the process for W_t is

$$\begin{aligned} \frac{dW_t}{W_t} &= p \frac{dS_t}{S_t} + (1-p) \frac{dB_t}{B_t} \\ &= (r + p(\mu - r)) dt + p\sigma dZ. \end{aligned} \quad (2.3)$$

98 Given an initial investment W_0 at $t = 0$, with terminal wealth W_T , we can pose the problem of
 99 determining the optimal control $p(W_t, t), t \in [0, T]$ in terms of a mean-variance objective. Defining
 100 a scalarization parameter $\kappa > 0$, the mean-variance problem can be formulated as

$$\sup_{p(\cdot)} E[W_T] - \kappa \text{Var}[W_T]. \quad (2.4)$$

101 Varying κ in equation (2.4) traces out the efficient frontier. Problem (2.4) cannot be solved di-
 102 rectly using dynamic programming. From (Zhou and Li, 2000; Li and Ng, 2000), we learn that we

103 can determine the control $p(\cdot)$ which maximizes objective function (2.4) by solving the alternative
 104 problem

$$\inf_{p(\cdot)} E[(W^* - W_T)^2], \quad (2.5)$$

105 where we trace out the efficient frontier by varying W^* . Note that Problem 2.5 can be solved using
 106 dynamic programming.¹

The optimal control for Problem 2.5 is given by (Zhou and Li, 2000; Li and Ng, 2000; Vigna, 2014)

$$p = \frac{\xi}{\sigma W_t} \left(W^* e^{-r(T-t)} - W_t \right)$$

where $\xi = \frac{\mu - r}{\sigma}$. (2.6)

Let W_T^{opt} denote the terminal wealth under strategy (2.6). The efficient frontier is then given by (Zhou and Li, 2000; Li and Ng, 2000)

$$\begin{aligned} E[W_T^{opt}] &= W_0 e^{rT} + \left(e^{\xi^2 T} - 1 \right)^{1/2} \sqrt{\text{Var}(W_T^{opt})} \\ &= W_0 e^{rT} + \left(e^{\xi^2 T} - 1 \right)^{1/2} \text{std}(W_T^{opt}). \end{aligned} \quad (2.7)$$

107 where $\text{Var}[\cdot]$ denotes variance.

108 Recall that varying W^* will move us along the efficient frontier. Since equation (2.7) is a
 109 monotone increasing function of variance, for a fixed value of $E[W_T^{opt}]$ the strategy which minimizes
 110 $\text{Var}(W_T^{opt})$ also minimizes $\text{std}(W_T^{opt})$. Consequently, from equations (2.1) and (2.7), the optimal
 111 Sharpe ratio is

$$\mathbb{S}^{opt} = \left(e^{\xi^2 T} - 1 \right)^{1/2}. \quad (2.8)$$

On the other hand, suppose we rebalance to a constant weight, i.e. $p = \text{const.}$ in equation (2.3). Let W_T^p denote the terminal wealth under a constant weight strategy p . Then we have

$$\begin{aligned} E[W_T^p] &= W_0 e^{(p(\mu-r)+r)T} \\ \text{std}[W_T^p] &= E[W_T^p] \left(e^{(\sigma p)^2 T} - 1 \right)^{1/2}, \end{aligned} \quad (2.9)$$

with Sharpe ratio

$$\begin{aligned} \mathbb{S}^p &= \frac{1 - e^{-p(\mu-r)T}}{\left(e^{(\sigma p)^2 T} - 1 \right)^{1/2}} \\ &\simeq \xi \sqrt{T} = \frac{(\mu - r) \sqrt{T}}{\sigma}; \quad T \rightarrow 0 \text{ or } p \rightarrow 0. \end{aligned} \quad (2.10)$$

112 Note that the continuously compounded Sharpe ratio is a function of p in general, and approaches
 113 the instantaneous Sharpe ratio only in the limit as $T \rightarrow 0$ or $p \rightarrow 0$.

¹In Vigna (2014), it is shown that $W_t < W^*$, $\forall t$ under the optimal control.

114 Let

$$E[W_T^{opt,p}] = W_0 e^{rT} + \left(e^{\xi^2 T} - 1 \right)^{1/2} std(W_T^p) . \quad (2.11)$$

115 This can be interpreted as follows. Given a constant weight strategy with equity fraction p ,
116 which generates $std(W_T^p)$, $E[W_T^{opt,p}]$ is the expected terminal wealth under control (2.6) which has
117 the same the standard deviation $std(W_T^p)$ (this follows from equation (2.7)).

118 A convenient way to compare these strategies is through the *apparent* annualized α , which we
119 define as

$$\alpha^p = \frac{\log(E[W_T^{opt,p}]) - \log(E[W_T^p])}{T} . \quad (2.12)$$

120 This is the extra annualized expected return generated by strategy (2.6) compared to the constant
121 weight strategy with equity fraction p , given that both strategies have the same risk, as measured
122 by standard deviation. Consistent with Goetzmann et al. (2002), we call α^p the apparent alpha,
123 since there is no stock-picking skill involved here, merely use of a dynamic control.

124 Before proceeding to some illustrative numerical examples, we note that the MV optimal strategy
125 with control (2.6) does not restrict the equity weight p in any way, permitting unlimited leverage
126 and short-selling. As a result, the strategy is typically very aggressive, with heavy use of leverage
127 early on. However, a rigorous solution of Problem 2.4 with no-shorting and no-leverage constraints
128 requires numerical solution of a Hamilton-Jacobi-Bellman (HJB) equation (Wang and Forsyth,
129 2010). It is more instructive for our purposes to approximate the constrained control using the
130 approach in Vigna (2014). We constrain the unconstrained control so that there is no-shorting and
131 no-leverage, by letting p^* be the unconstrained solution to (2.6) and setting

$$p = \max(0.0, \min(p^*, 1.0)) . \quad (2.13)$$

132 In the following, we will refer to the strategy that uses this constrained approach as the Clipped
133 MV Optimal strategy, in contrast to the unconstrained MV Optimal strategy (2.6).

134 We conclude this section with a couple of comments about options trading and pre-commitment
135 and time consistency. With regard to options, we note that any portfolio that uses covered call
136 writing (or equivalently, cash-secured put writing) can be replicated by continuous trading in a
137 portfolio which has a risk-free bond and the underlying stock that satisfies the no-shorting, no-
138 leverage constraints as in the Clipped MV Optimal strategy (see Appendix A). More generally, in
139 the complete market case dynamic trading in the bond and stock is equivalent to using options in the
140 trading strategy. Hence, even if options are not directly included in, for example, the MV Optimal
141 strategy (2.6), this is clearly equivalent to the use of derivatives. As a result, we can think of any
142 financial product based on a dynamic trading strategy as a structured product. In the presence of
143 constraints, the market may be incomplete. However, with some abuse of common terminology, we
144 will still refer to such packaged investment vehicles as structured products, even in an incomplete
145 market.

146 With respect to pre-commitment and time consistency, we make the following two observations:

147 **Remark 2.1** (Pre-commitment policy). *Strategy (2.6) is the pre-commitment solution, which is not*
148 *formally time consistent. However, consider the case of a retail investor, who purchases a financial*
149 *product from a financial institution. The investor does not trade herself in the assets underlying*
150 *the product during the life of the contract. Hence, the performance of the product is evaluated in*
151 *terms of the initial and final wealth. Consequently, as noted in Bernard and Vanduffel (2014), the*
152 *pre-commitment policy is appropriate in this case.*

153 **Remark 2.2** (Pre-commitment strategies equivalence to induced time consistent strategy). *The*
154 *control (2.6) is formally the pre-commitment policy. However, the time zero strategy based on*
155 *the pre-commitment policy solution of Problem 2.4 is identical to the strategy for an induced time*
156 *consistent policy, and hence it is implementable.² The induced time consistent strategy in this case*
157 *is a target based shortfall, Problem 2.5, with a fixed value of $W^* \forall t > 0$. The concept of induced time*
158 *consistent strategies is discussed in Strub et al. (2019). The relationship between pre-commitment*
159 *and implementable target-based schemes in the mean-variance context is discussed in Vigna (2014;*
160 *2022) and Menoncin and Vigna (2017).*

161 2.1 Numerical Examples

162 We use data from the Center for Research in Security Prices (CRSP) on a monthly basis over
163 the 1926:1-2019:12 period.³ Our base case tests use the CRSP 30 day T-bill for the bond asset
164 and the CRSP value-weighted total return index for the stock asset. This latter index includes all
165 distributions for all domestic stocks trading on major U.S. exchanges. All of these various indexes
166 are in nominal terms, so we adjust them for inflation by using the U.S. CPI index (also obtained
167 from CRSP). Since we are considering a multi-year investment horizon, it is important to use real
168 (i.e. inflation-adjusted) returns.

169 With constant parameters, specification (2.2) assumes geometric Brownian motion with drift
170 μ and volatility σ for the stock index, and a constant risk-free rate r . Table 2.1 gives maximum
171 likelihood estimates for μ and σ , as well as the long-run sample average value of the 30 day T-bill
172 rate which we take as a proxy for r . This table also summarizes our investment scenario, with initial
173 wealth $W_0 = 1000$, an investment horizon of $T = 5$ years, and monthly rebalancing.

Stochastic Model Parameters		Investment Scenario	
μ	.0822	W_0	1000
σ	.1842	T	5 years
r	.0044	Rebalancing	Monthly

TABLE 2.1: *Investment scenario and estimated annualized parameters for processes (2.2), based on inflation-adjusted value-weighted CRSP index and 30 day T-bills. Sample period 1926:1 to 2019:12.*

174 The illustrative examples both here and in subsequent sections of the paper are based on two
175 different simulation procedures. The first, which we call the synthetic market, uses standard Monte
176 Carlo simulation techniques for asset returns, assuming that the model is correctly specified (i.e.
177 in this case, we simulate geometric Brownian motion for stock index returns with $\mu = .0822$ and
178 $\sigma = .1842$, and we set the risk-free rate r to the constant value of .0044). The second simulation
179 procedure, which we refer to as the historical market, relies on the stationary block bootstrap
180 method (Politis and Romano, 1994; Politis and White, 2004; Patton et al., 2009; Dichtl et al., 2016).
181 In particular, we use monthly resampled returns from the historical data set, with data drawn with
182 replacements in blocks of various sizes simultaneously for the stock and bond indexes. Sampling the
183 data in blocks incorporates potential serial correlation in the real return data. The block sizes are

²An implementable strategy has the property that the investor has no incentive to deviate from the strategy computed at time zero at later times (Forsyth, 2020a).

³More specifically, results presented here were calculated based on data from Historical Indexes, ©2020 Center for Research in Security Prices (CRSP), the University of Chicago Booth School of Business. Wharton Research Data Services was used in preparing this article. This service and the data available thereon constitute valuable intellectual property and trade secrets of WRDS and/or its third-party suppliers.

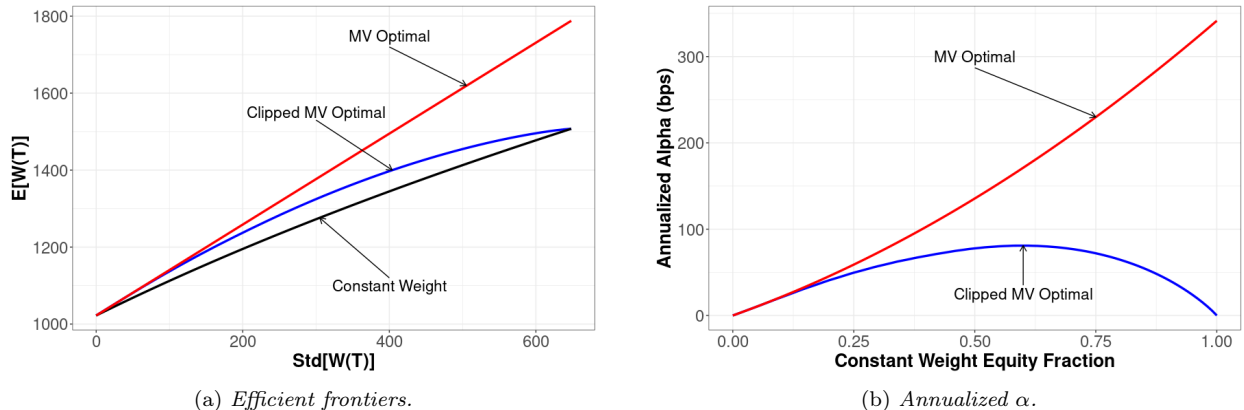


FIGURE 2.1: Comparison of constant weight and MV optimal strategies in the synthetic market with 640,000 paths and parameters from Table 2.1.

184 randomly drawn, based on an expected blocksize parameter $\hat{b} = 1/v$ where the block size follows
 185 a geometric distribution with $Prob(b = k) = (1 - v)^{k-1}v$. Enough blocks are then pasted together
 186 to construct simulated paths over the investment horizon of $T = 5$ years. The optimal value of \hat{b}
 187 can be estimated using an algorithm from Patton et al. (2009). However, applying this algorithm
 188 separately to the real stock index and 30-day T-bill series results in quite different estimates: about
 189 3 months for the former, and 50 months for the latter. If we take the average estimate from the
 190 two series, we get about two years. However, we provide results for a range of expected blocksizes
 191 as a check on the robustness of the historical market results. We emphasize that these historical
 192 market simulations make no assumptions about the stochastic processes governing bond and stock
 193 index returns.⁴

194 Figure 2.1 shows synthetic market results for constant weight strategies (with $p \in [0,1]$), along
 195 with MV Optimal and Clipped MV Optimal strategies, with 640,000 paths and monthly rebalancing.
 196 Panel (a) plots the efficient frontiers, i.e. $E[W_T]$ vs. $std[W_T]$. Given that the risk-free rate is
 197 assumed to be non-stochastic, it is possible to achieve a standard deviation of zero by investing
 198 entirely in the risk-free asset. The Clipped MV Optimal strategy is clearly constrained to match
 199 the constant weight strategy for constant equity weights of both $p = 0$ and $p = 1$, but it offers some
 200 outperformance compared to the constant weight strategy using intermediate values of p . The MV
 201 Optimal strategy provides strong outperformance, particularly for high levels of risk as measured
 202 by standard deviation. Panel (b) plots the annualized alpha (2.12) in bps for the MV Optimal and
 203 Clipped MV Optimal strategies, relative to constant weight strategies. The MV Optimal strategy
 204 gives very high apparent alpha (over 300 bps) as the constant equity weight approaches 1, but
 205 this unconstrained strategy is arguably quite unrealistic, having no limit whatsoever on leverage.
 206 In contrast, the Clipped MV Optimal strategy gives a maximum apparent alpha of about 80 bps
 207 relative to a constant weight strategy with $p \approx 0.6$, but as noted above the constraints imposed
 208 imply that the Clipped MV Optimal strategy cannot offer any outperformance compared to using
 209 a constant weight of $p = 1$.⁵

⁴Detailed pseudo-code for block bootstrap resampling can be found in Forsyth and Vetzal (2019).

⁵The results provided in Figure 2.1 are based on monthly rebalancing and 640,000 paths, but the actual control for the MV Optimal strategy (2.6) assumes continuous rebalancing. Obviously, in practice rebalancing must be discrete. Additional simulations were run increasing the number of paths by a factor of 4 and increasing the rebalancing frequency to 10 times per month. The expected value of terminal wealth and its standard deviation in all cases changed by less than 1% from the values given in Figure 2.1(a). Somewhat larger changes (up to almost 5%) were observed for the apparent alphas in Figure 2.1(b), in cases where there was a significant equity weight.

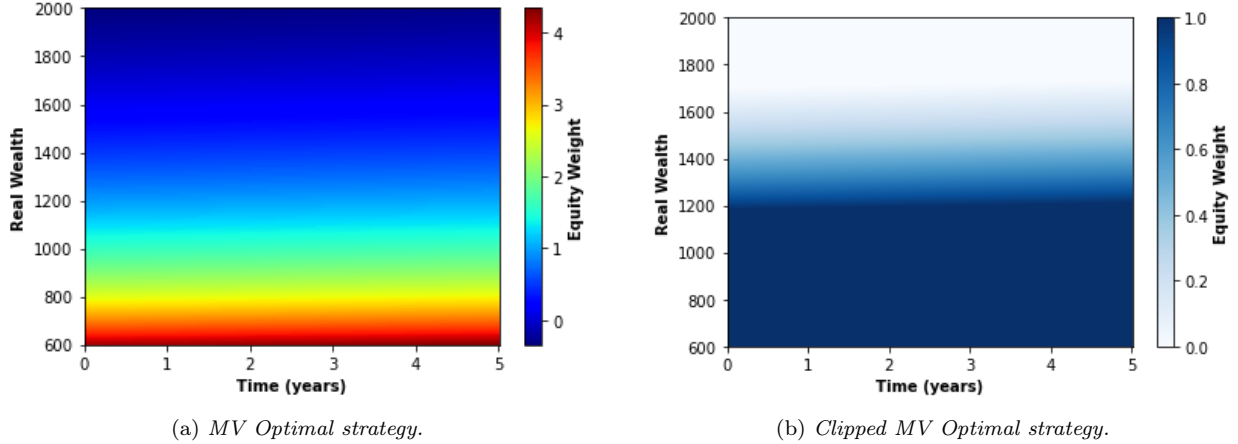


FIGURE 2.2: Heatmaps of optimal equity weights based on parameters from Table 2.1 with $W^* = 1736$.

210 The MV Optimal control (2.6) depends on time only through the present value factor $e^{-r(T-t)}$.
 211 Since we are working in real terms and the long run real interest rate r at .0044 is not much above
 212 zero, the control strategy at any point in time should depend almost entirely on the level of real
 213 wealth then. This is seen in Figure 2.2, which provides heatmaps indicating the optimal fraction
 214 invested in equities at various wealth levels over the 5-year investment horizon for the MV Optimal
 215 and Clipped MV Optimal strategies.⁶ The contrarian behavior of these strategies alluded to above
 216 is clear from both panels of Figure 2.2, as the portfolio has reduced equity exposure for high levels
 217 of real wealth, which would follow from strong prior market returns. Conversely, the strategies
 218 increase equity exposure at low real wealth, which would result from poor previous returns. The
 219 two panels are plotted with different color scales to highlight the extremely aggressive nature of
 220 the MV Optimal strategy. At the initial level $W_0 = 1000$ the equity weight is about 1.60, and this
 221 would increase to more than 4 if real wealth were to decline by about 40%.⁷

222 Further insight into the properties of both MV optimal strategies can be gleaned from examining
 223 the evolution of the densities of real wealth over time, as shown in Figure 2.3. These plots use the
 224 same W^* of 1763 with 640,000 paths and monthly rebalancing, although the densities are plotted
 225 on a quarterly basis. In addition to the densities, both plots show a single vertical black line at
 226 $W_0 = 1000$, as well as three colored vertical lines, which mark the 5th, 50th, and 95th percentiles of
 227 the distribution at each point in time shown. Since we are rebalancing discretely, there is a non-zero
 228 probability of exceeding W^* . Both strategies have a large left skew. This is particularly true for
 229 the MV Optimal strategy in panel (a). In contrast, the Clipped MV Optimal strategy in panel (b)
 230 cuts off part of the extreme left tail.

231 We next consider historical market simulations. Recall that this entails resampling from the
 232 actual observed data, rather than a Monte Carlo simulation of the assumed stochastic model. We
 233 again use 640,000 paths, and start by considering an expected blocksize of 60 months. Figure 2.4
 234 is analogous to Figure 2.1 above, showing efficient frontiers and apparent alpha. In this case, there
 235 are some non-Pareto optimal points which have been removed for plotting purposes. For example,
 236 the frontier for the constant weight strategy in panel (a) bends back, with higher $std[W_T]$ and lower
 237 $E[W_T]$ if we consider weights closer to zero. Unlike the synthetic market with a constant interest
 238 rate where risk could be pushed all the way to zero, that is impossible here since the interest rate

⁶Here we specify $W^* = 1736$, a value which results in the Clipped MV Optimal strategy having $std[W_T]$ that is approximately equal to that produced by a constant weight strategy with $p = 0.6$.

⁷Note that control (2.6) implies that leverage is unbounded as $W_t \rightarrow 0^+$.

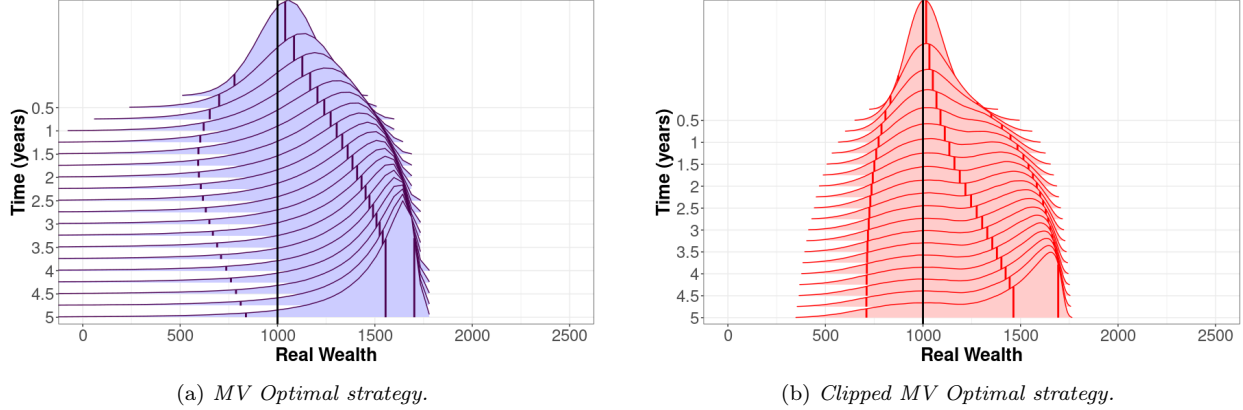


FIGURE 2.3: Densities of real wealth over time based on data from Table 2.1 with $W^* = 1736$, 640,000 simulated synthetic market paths, and monthly rebalancing. Densities plotted quarterly. The black vertical line indicates the initial real wealth $W_0 = 1000$. The colored vertical lines in each density represent the 5th, 50th, and 95th percentiles of the distribution.

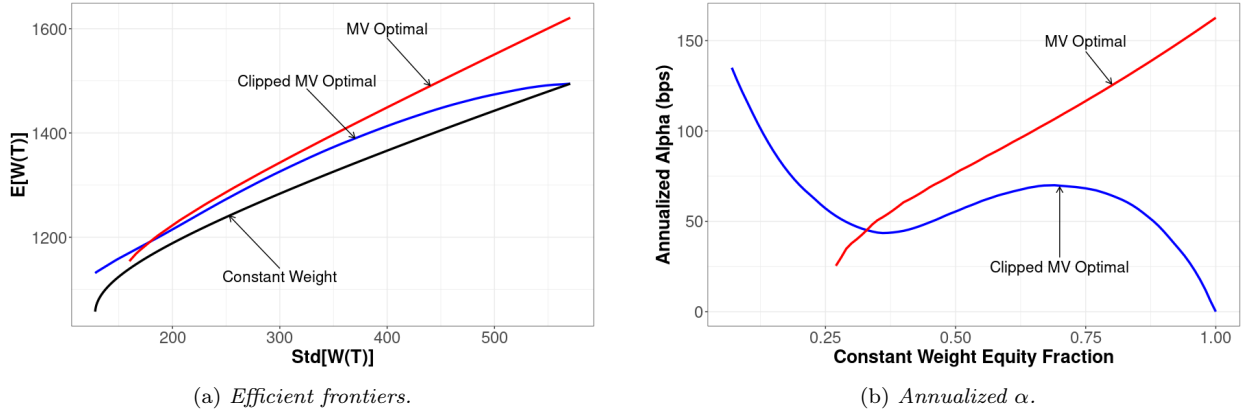


FIGURE 2.4: Comparison of constant weight and MV optimal strategies in the historical market with 640,000 paths, expected blocksize of 60 months, and parameters from Table 2.1. Non-Pareto optimal points removed for each strategy.

239 is stochastic. Panel (b) shows the expected alpha of zero for the Clipped MV Optimal strategy
 240 relative to the constant weight strategy with $p = 1$, and a corresponding significant alpha for the
 241 unconstrained MV Optimal strategy. However, this is much reduced from the level found in Fig-
 242 ure 2.1(b). Panel (b) also indicates high alpha for the Clipped MV Optimal strategy compared
 243 to constant weight strategies that are heavily invested in bonds, but from panel (a) this is largely
 244 because the constant weight strategy performs poorly in these cases. As might be expected, the
 245 performance of the two MV Optimal strategies is worse under the conditions of these historical mar-
 246 ket tests, relative to the synthetic market which uses return data based on the geometric Brownian
 247 motion model that is assumed when deriving the control strategy.

248 These conclusions are reinforced by Figure 2.5, which repeats the exercise but this time draws
 249 the historical data using an expected blocksize of 24 months. This is an even more stringent test,
 250 since there can be many paths with very large changes in interest rates. For example, a period
 251 of sampling from the early 1980s when interest rates were very high may be followed on the same
 252 simulated path by a stretch of sampling from the 2010s when interest rates were quite low. While
 253 this type of situation could happen with the larger expected blocksize of 60 months considered

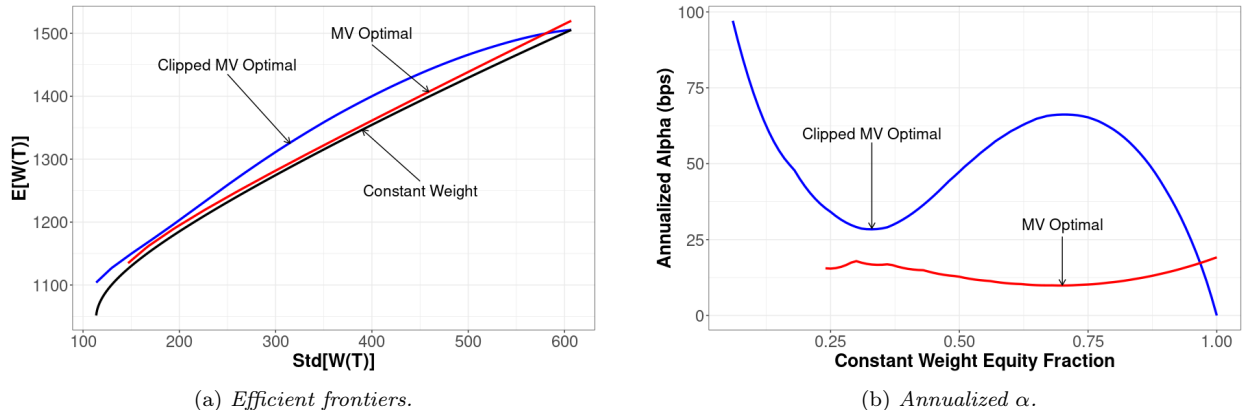


FIGURE 2.5: Comparison of constant weight and MV optimal strategies in the historical market with 640,000 paths, expected blocksize of 24 months, and parameters from Table 2.1. Non-Pareto optimal points removed for each strategy.

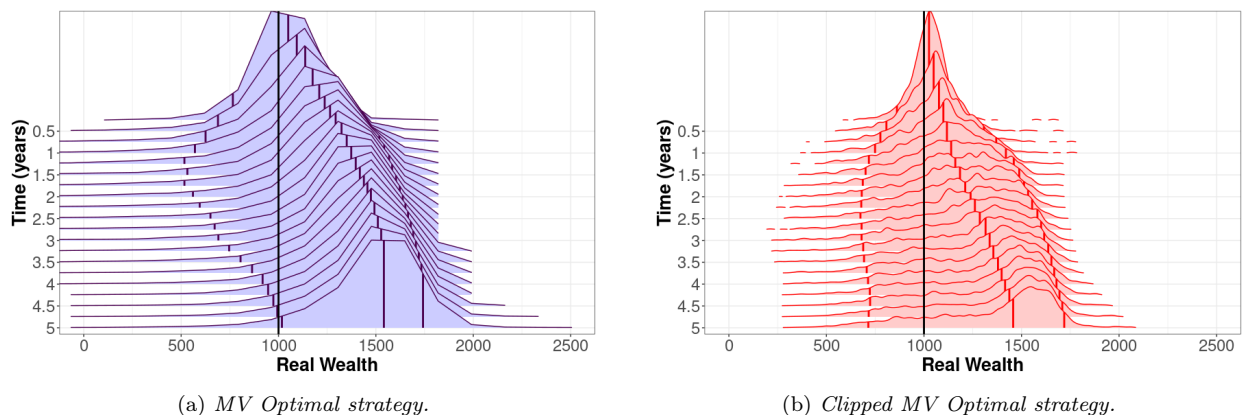


FIGURE 2.6: Densities of real wealth over time based on data from Table 2.1 with $W^* = 1736$, 640,000 simulated historical market paths, expected blocksize of 60 months, and monthly rebalancing. Densities plotted quarterly. The black vertical line indicates the initial real wealth $W_0 = 1000$. The colored vertical lines in each density represent the 5th, 50th, and 95th percentiles of the distribution.

254 above, it is much more likely here with the shorter expected blocksize. Compared to Figure 2.4,
 255 we observe even worse performance, especially for the MV Optimal strategy. In fact, here the MV
 256 Optimal strategy is worse than the Clipped MV Optimal strategy, except for cases with very high
 257 $std[W_T]$. We conjecture that this is because the aggressive nature of the MV Optimal strategy
 258 makes it more sensitive to model mis-specification.

259 Finally, in Figure 2.6 we show the evolution of the density of real wealth over time for the MV
 260 strategies, in the historical market with an expected blocksize of 60 months. While there are obvious
 261 general similarities with the corresponding Figure 2.3 in the synthetic market, we can observe that
 262 the real wealth densities are not as smooth here, and the chance of achieving higher real final wealth
 263 is increased. This is because the strategy of de-risking is still based on the assumption of constant
 264 interest rates, but here rates are stochastic (i.e. there are cases where the de-risked portfolio earns
 265 higher than expected returns, leading to higher final wealth).

2.2 Deficiencies of MV (Sharpe Ratio) Criteria

The apparent alpha generated by an MV optimal strategy comes from skewing the terminal wealth distribution. The right side of the distribution is cut-off (eliminating very large gains), and at the same time, an increase in left tail risk occurs (Lhabitant, 2000; Goetzmann et al., 2002; Forsyth and Vetzal, 2017a;b; 2019). As shown above in the synthetic market Figure 2.3, the left tail risk is somewhat reduced when constraints are imposed. This can also be seen as a natural consequence of the contrarian flavor of the strategy, which increases the weight in stocks when wealth decreases, and decreases the weight in stocks when wealth increases, i.e. buy when the market goes down, sell when the market goes up (see Figure 2.2). This implies that the investor is fully invested in bonds after stocks do well, and will not participate in further gains. On the other hand, the investor increases holdings in stocks when stocks perform poorly. This means that poor results can be expected if the market trends downward over the entire investment horizon. In this case (downward trending stocks in $[0, T]$) control (2.6) will generate a worse result than a constant weight strategy, which keeps at least some proportion of wealth always invested in bonds. The opposite is true at large values of wealth. In this case, an MV optimal strategy is always fully invested in bonds, while the constant weight strategy has some investment in stocks, and can participate in further equity market gains.

In summary, we can see that a major problem with dynamic MV (Sharpe ratio maximizing) strategies is that variance is a symmetric risk measure, which penalizes both the upside as well as the downside. An easy way to improve Sharpe ratios is to sell off the upside, which trivially reduces variance. On the other hand, somewhat counterintuitively, Sharpe ratio maximizing strategies also increase left tail risk, compared to a benchmark constant weight strategy.⁸ This motivates us to consider below strategies that rely on a downside risk measure. In addition, the results above show the potential importance of imposing constraints: the MV Optimal strategy uses large amounts of leverage, which is unrealistic. However, below we specify constraints directly as part of the optimization problem, rather than being imposed afterwards in an ad hoc manner, as in (2.13).

3 Mean-Expected Shortfall Strategies

Based on our analysis of dynamic MV strategies, it seems clear that an asymmetric risk measure might be more useful than variance. If we directly target an asymmetric risk measure in the objective function, this will shape the distribution of the terminal wealth in a way which corresponds to our intuitive concept of risk (i.e. downside not upside).

Let $g(W_T)$ be the probability density function of terminal wealth W_T at $t = T$, and let

$$\int_{-\infty}^{W_\beta^*} g(W_T) dW_T = \beta, \quad (3.1)$$

so that $Prob[W_T > W_\beta^*] = 1 - \beta$. We can interpret W_β^* as the Value at Risk (VAR) at level β . The Expected Shortfall (ES) at level β is then

$$ES_\beta = \frac{\int_{-\infty}^{W_\beta^*} W_T g(W_T) dW_T}{\beta}, \quad (3.2)$$

which is the mean of the worst β fraction of outcomes. Typically, $\beta \in \{.01, .05\}$. Note that the definition of ES in equation (3.2) uses the probability density of the final wealth distribution, not

⁸Note that in some cases an asset allocation strategy based on objective function (2.4) may be desirable based on the CDF of the final wealth distribution (see, e.g. Forsyth and Vetzal, 2019). However, this is best understood in terms of objective function (2.5), rather than Sharpe ratio maximization.

301 the density of *loss*. Hence, in our case a larger value of ES (i.e. a larger value of average worst
 302 case terminal wealth) is desired.⁹ It will be convenient to use the equivalent definition of ES_β from
 303 Rockafellar and Uryasev (2000):

$$ES_\beta = \sup_{W^*} E \left[W^* + \frac{\min(W_T - W^*, 0)}{\beta} \right]. \quad (3.3)$$

304 As a measure of reward, we will simply use expected wealth $E[W_T]$, denoted by EW. Since
 305 ES_β and EW are conflicting measures, we find Pareto optimal strategies by using a scalarization
 306 parameter $\kappa > 0$ and then maximizing the objective function

$$ES_\beta + \kappa EW. \quad (3.4)$$

307 Varying κ traces out an efficient frontier in the (EW, ES) plane.

308 We will determine optimal strategies which are discretely rebalanced with no-shorting and no-
 309 leverage constraints. We next outline our assumptions concerning the stochastic processes of the
 310 underlying investments and some notational conventions.

311 4 Investment Market

312 We assume that the investor has access to two funds: a broad market stock index fund and a
 313 constant maturity bond index fund. The investment horizon is T . Let S_t and B_t respectively
 314 denote the real amounts invested in the stock index and the bond index respectively. In general,
 315 these amounts will depend on the investor's strategy as well as changes in the real unit prices of
 316 the assets. In the absence of an investor determined control (i.e. cash injections or rebalancing), all
 317 changes in S_t and B_t result from changes in asset prices.

318 We model the stock index as following a jump diffusion process. Let $S_{t-} = S(t - \epsilon)$, $\epsilon \rightarrow 0^+$, i.e.
 319 t^- is the instant of time before t , and let ξ^s be a random jump multiplier. When a jump occurs,
 320 $S_t = \xi^s S_{t-}$. We assume that $\log(\xi^s)$ follows a double exponential distribution (Kou, 2002; Kou and
 321 Wang, 2004). The probability of an upward jump is p_u^s , while $1 - p_u^s$ is the chance of a downward
 322 jump. The density function for $y = \log(\xi^s)$ is

$$f^s(y) = p_u^s \eta_1^s e^{-\eta_1^s y} \mathbf{1}_{y \geq 0} + (1 - p_u^s) \eta_2^s e^{\eta_2^s y} \mathbf{1}_{y < 0}. \quad (4.1)$$

323 Define

$$\kappa_\xi^s = E[\xi^s - 1] = \frac{p_u^s \eta_1^s}{\eta_1^s - 1} + \frac{(1 - p_u^s) \eta_2^s}{\eta_2^s + 1} - 1. \quad (4.2)$$

324 In the absence of control,

$$\frac{dS_t}{S_{t-}} = (\mu^s - \lambda_\xi^s \kappa_\xi^s) dt + \sigma^s dZ^s + d \left(\sum_{i=1}^{\pi_t^s} (\xi_i^s - 1) \right), \quad (4.3)$$

325 where μ^s is the (uncompensated) drift rate, σ^s is the diffusive volatility, Z^s is a Brownian motion, π_t^s
 326 is a Poisson process with positive intensity parameter λ_ξ^s , and ξ_i^s are i.i.d. positive random variables
 327 having distribution (4.1). Moreover, ξ_i^s , π_t^s , and Z^s are assumed to all be mutually independent.

328 In addition, we directly model the returns of the constant maturity bond index as a stochastic
 329 process, following MacMinn et al. (2014) and Lin et al. (2015). As in MacMinn et al. (2014), we

⁹The negative of ES is often called Conditional Value at Risk (CVAR).

330 assume that the constant maturity bond index follows a jump diffusion process, similar in form
 331 to the process assumed above for the stock index. In particular, $B_{t-} = B(t - \epsilon), \epsilon \rightarrow 0^+$. In the
 332 absence of control, B_t evolves as

$$\frac{dB_t}{B_{t-}} = \left(\mu^b - \lambda_\xi^b \kappa_\xi^b + \mu_c^b \mathbf{1}_{\{B_{t-} < 0\}} \right) dt + \sigma^b dZ^b + d \left(\sum_{i=1}^{\pi_t^b} (\xi_i^b - 1) \right), \quad (4.4)$$

333 where the terms in equation (4.4) are defined analogously to equation (4.3). In particular, π_t^b is a
 334 Poisson process with positive intensity parameter λ_ξ^b , and ξ_i^b has distribution

$$f^b(y = \log \xi^b) = p_u^b \eta_1^b e^{-\eta_1^b y} \mathbf{1}_{y \geq 0} + (1 - p_u^b) \eta_2^b e^{\eta_2^b y} \mathbf{1}_{y < 0}, \quad (4.5)$$

335 and $\kappa_\xi^b = E[\xi^b - 1]$. ξ_i^b , π_t^b , and Z^b are assumed to all be mutually independent. The term
 336 $\mu_c^b \mathbf{1}_{\{B_{t-} < 0\}}$ in equation (4.4) represents an additional cost of borrowing ($B_t < 0$), i.e. a spread
 337 between borrowing and lending rates. We assume that the diffusive components of S_t and B_t are
 338 correlated, i.e. $dZ^s \cdot dZ^b = \rho_{sb} dt$. However, the jump process terms for these two indexes are
 339 assumed to be mutually independent.¹⁰

340 By using jump processes and random interest rates, we have generalized the environment con-
 341 sidered in Section 2. In principle, equations (4.3) and (4.4) could be extended further to include
 342 stochastic volatility. However, Ma and Forsyth (2016) have shown that stochastic volatility is unim-
 343 portant if the time horizon of the investment is larger than the mean reversion time of the volatility
 344 process. Based on historical data, the half-life of a volatility shock is 1-2 months (Ma and Forsyth,
 345 2016). That said, we will conduct tests below similarly to Section 2.1: we will determine the opti-
 346 mal controls using the parametric model based on equations (4.3) and (4.4), and then apply these
 347 controls both in the synthetic market (i.e. with Monte Carlo simulations of the same parametric
 348 model) and in the historical market, i.e. using resampled historical data, which is devoid of any
 349 specific assumptions about the underlying stochastic processes.

350 We define the investor's total wealth at time t as $W_t \equiv S_t + B_t$. We generally impose the
 351 constraints that (assuming solvency) shorting stock and using leverage (i.e. borrowing) are not
 352 allowed, However, in some of our examples we will allow limited use of leverage. In such cases, we
 353 assume that the cost of borrowing is the return of the constant maturity bond index plus the spread
 354 component μ_c^b .

355 5 Notational Conventions

356 We specify a set of discrete rebalancing times \mathcal{T}

$$\mathcal{T} = \{t_0 = 0 < t_1 < t_2 < \dots < t_M = T\} \quad (5.1)$$

357 where it is assumed that $t_i - t_{i-1} = \Delta t = T/M$ is constant for simplicity. To reduce subscripts,
 358 we will sometimes use the notation $S_t \equiv S(t), B_t \equiv B(t)$ and $W_t \equiv W(t)$. More specifically, let
 359 the inception time of the investment be $t_0 = 0$. At each time $t_i, i = 0, 1, \dots, M - 1$, the investor
 360 rebalances the portfolio. At $t_M = T$, the portfolio is liquidated.

361 Given a time dependent function $f(t)$, we will use the shorthand notation $f(t_i^+) \equiv \lim_{\epsilon \rightarrow 0^+} f(t_i + \epsilon)$
 362 and $f(t_i^-) \equiv \lim_{\epsilon \rightarrow 0^+} f(t_i - \epsilon)$.

¹⁰See Forsyth (2020b) for a discussion of the evidence for stock and bond price jump independence.

363 We assume no taxes are triggered on rebalancing.¹¹ We also assume that transaction costs are
 364 small enough to be ignored in our analysis. This is not unreasonable as we assume discrete and
 365 relatively infrequent rebalancing, and we can also imagine that the investor holds units of a large
 366 pooled contract. In addition, the basic underlying investments are assumed to be broad stock and
 367 bond index ETFs, which are very liquid. This then implies that the condition

$$W(t_i^+) = W(t_i^-) \quad (5.2)$$

368 holds.¹²

369 The multi-dimensional controlled underlying process is denoted $X(t) = (S(t), B(t))$, with $t \in$
 370 $[0, T]$. The realized state of the system is $x = (s, b)$. Let the rebalancing control $p_i(\cdot)$ be the fraction
 371 invested in the stock index at rebalancing date t_i , i.e.

$$p_i(X(t_i^-)) = p(X(t_i^-), t_i) = \frac{S(t_i^+)}{S(t_i^+) + B(t_i^+)}. \quad (5.3)$$

The controls depend on the state of the investment portfolio before the rebalancing occurs, i.e.
 $p_i(\cdot) = p(X(t_i^-), t_i) = p(X_i^-, t_i)$, $t_i \in \mathcal{T}$, the set of rebalancing times. We determine the optimal
 strategies amongst all strategies with constant wealth (before and after rebalancing), so that

$$\begin{aligned} p_i(\cdot) &= p(W(t_i^+), t_i) \\ W(t_i^+) &= S(t_i^-) + B(t_i^-) \\ S(t_i^+) &= S_i^+ = p_i(W_i^+) W_i^+ \\ B(t_i^+) &= B_i^+ = (1 - p_i(W_i^+)) W_i^+. \end{aligned} \quad (5.4)$$

372 Let \mathcal{Z} represent the set of admissible values of the control $p_i(\cdot)$. An admissible control $\mathcal{P} \in \mathcal{A}$,
 373 where \mathcal{A} is the admissible control set, can be written as

$$\mathcal{P} = \{p_i(\cdot) \in \mathcal{Z} : i = 0, \dots, M-1\}. \quad (5.5)$$

374 No-shorting and no-leverage constraints are imposed by specifying

$$\mathcal{Z} = [0, 1]. \quad (5.6)$$

375 Finally, we define $\mathcal{P}_n \equiv \mathcal{P}_{t_n} \subset \mathcal{P}$ as the tail of the set of controls in $[t_n, t_{n+1}, \dots, t_{M-1}]$, i.e.

$$\mathcal{P}_n = \{p_n(\cdot), \dots, p_{M-1}(\cdot)\}. \quad (5.7)$$

376 6 Problem Definition

377 We now specify the EW-ES problem which was discussed informally in Section 3. Since expected
 378 wealth (EW) and expected shortfall (ES) are conflicting measures, we use a scalarization technique
 379 to find the Pareto points for this multi-objective optimization problem. For a given scalarization
 380 parameter $\kappa > 0$, we seek the control \mathcal{P}_0 that maximizes

$$\text{ES}_\beta(X_0^-, t_0^-) + \kappa \text{EW}(X_0^-, t_0^-). \quad (6.1)$$

¹¹If the contract is held in a tax-advantaged savings account, then no taxes are paid on rebalancing. In addition, in Canada rebalancing can occur without triggering taxes in a corporate class mutual fund. In the US, ETFs can defer taxes on rebalancing through the use of *heartbeat* trades (Moussawi et al., 2022).

¹²Transaction costs can be incorporated with increased computational cost. In addition, large liquid ETFs have very low transaction costs, which have little effect with infrequent trading (van Staden et al., 2018).

More precisely, we define the pre-commitment EW-ES problem ($PCEE_{t_0}(\kappa)$) problem in terms of the value function $J(s, b, t_0^-)$, where we use the definition of ES_β from equation (3.3).

$$(PCEE_{t_0}(\kappa)) : \quad J(s, b, t_0^-) = \sup_{\mathcal{P}_0 \in \mathcal{A}} \sup_{W^*} \left\{ E_{\mathcal{P}_0}^{X_0^+, t_0^+} \left[W^* + \frac{1}{\beta} \min(W_T - W^*, 0) + \kappa W_T \right. \right. \\ \left. \left. \left| X(t_0^-) = (s, b) \right. \right] \right\} \quad (6.2)$$

$$\text{subject to } \begin{cases} (S_t, B_t) \text{ follow processes (4.3) and (4.4); } t \notin \mathcal{T} \\ W_\ell^+ = S_\ell^- + B_\ell^-; X_\ell^+ = (S_\ell^+, B_\ell^+) \\ S_\ell^+ = p_\ell(\cdot)W_\ell^+; B_\ell^+ = (1 - p_\ell(\cdot))W_\ell^+ \\ p_\ell(\cdot) \in \mathcal{Z}(W_\ell^+, t_\ell) \\ \ell = 0, \dots, M; t_\ell \in \mathcal{T} \end{cases} \quad (6.3)$$

381 Interchange the sup sup¹³ in equation (6.2), so that value function $J(s, b, t_0^-)$ can be written as
382

$$J(s, b, t_0^-) = \sup_{W^*} \sup_{\mathcal{P}_0 \in \mathcal{A}} \left\{ E_{\mathcal{P}_0}^{X_0^+, t_0^+} \left[W^* + \frac{1}{\beta} \min(W_T - W^*, 0) + \kappa W_T \left| X(t_0^-) = (s, b) \right. \right] \right\}. \quad (6.4)$$

383 Appendix B notes that the control determined from the pre-commitment policy (6.4) at time
384 zero is identical to the control determined from a time consistent linear shortfall policy. However, as
385 discussed in Section 2, the pre-commitment strategy is appropriate for a financial product purchased
386 by a retail customer, and we will not discuss the induced time consistent policy further. We use the
387 method described in Forsyth (2020a) to solve Problem 6.2. For the convenience of the reader, we
388 provide a brief description of this method in Appendix C.

389 7 Parameter Estimates and Investment Scenario

390 We estimate the parameters for the double exponential jump diffusion processes (4.3) and (4.4)
391 using the data described in Section 2.1. Recall that this is monthly data from 1926 to 2019 for
392 inflation-adjusted returns for the CRSP value-weighted total return and 30-day US T-bill indexes.
393 We use the threshold technique (Mancini, 2009; Cont and Mancini, 2011; Dang and Forsyth, 2016).
394 Table 7.1 shows the results of calibrating the models to the historical data. The correlation ρ_{sb} is
395 computed by removing any returns which occur at times corresponding to jumps in either series,
396 and then using the sample covariance. Further discussion of the validity of assuming that the stock
397 and bond jumps are independent is given in Forsyth (2020b).

398 Table 7.2 shows our base case investment scenario. We consider $T = 5$ years, with an initial
399 investment of 1000. Rebalancing occurs discretely, on a quarterly basis. Our default constraints
400 (see equation (5.5)) are $\mathcal{Z} = [0, 1]$, i.e. no shorting and no-leverage. This clearly implies that no
401 trading occurs under insolvency, which can only occur if there is a jump to zero for both assets. In
402 Table 7.2 we have set the borrowing spread $\mu_c^b = .02$. There is no borrowing in our base case, but
403 we do allow leverage in some of our later examples.

¹³Let $F = \sup_{(a,b) \in A \times B} f(a,b)$, then $\forall \epsilon > 0, \exists (a^*, b^*) \in A \times B$, s.t. $f(a^*, b^*) > F - \epsilon$. Then $F \geq \sup_{a \in A} \sup_{b \in B} f(a,b) \geq \sup_{b \in B} f(a^*, b) \geq f(a^*, b^*) > F - \epsilon$. Hence, $\epsilon \rightarrow 0$ implies $\sup_{a \in A} \sup_{b \in B} f(a,b) = F$. Similarly $\sup_{b \in B} \sup_{a \in A} f(a,b) = F$.

CRSP	μ^s	σ^s	λ^s	u^s	η_1^s	η_2^s	ρ_{sb}
	0.0877	0.1459	0.3191	0.2333	4.3608	5.504	0.08228
30-day T-bill	μ^b	σ^b	λ^b	u^b	η_1^b	η_2^b	ρ_{sb}
	0.0045	0.0130	0.5106	0.3958	65.85	57.75	0.08228

TABLE 7.1: *Estimated annualized parameters for double exponential jump diffusion model. Value-weighted CRSP index, 30 day US T-bill index deflated by the CPI. Sample period 1926:1 to 2019:12.*

Investment horizon T (years)	5.0
Equity market index	CRSP Cap-weighted index (real)
Bond index	30-day T-bill (US) (real)
Initial portfolio value W_0	1000
Rebalancing times	$t = 0, 0.25, 0.5, \dots, 4.5, 4.75$
Equity fraction range	$\mathcal{Z} \in [0, 1]$
Borrowing spread μ_c^b	0.02
Rebalancing interval (years)	0.25
Market parameters	See Table 7.1

TABLE 7.2: *Input data for examples.*

404 8 EW-ES alpha

405 Suppose we have a set of points $(E[W_T^{opt}], ES_\beta^{opt})$ on the efficient frontier, determined using the
406 optimal policy from Problem 6.2. In addition, we also compute points $(E[W_T^p], ES_\beta^p)$ with a constant
407 weight strategy p where p is the (constant) fraction in equities, reset at each discrete rebalancing
408 date. We can write the efficient EW-ES frontier, determined by solving Problem 6.3, as a function
409 $F(\cdot)$, i.e.

$$E[W_T^{opt}] = F(ES_\beta^{opt}). \quad (8.1)$$

410 For each value of p , we then determine

$$E[W_T^{opt,p}] = F(ES_\beta^p), \quad (8.2)$$

411 which is the expected wealth from the optimal strategy having the same risk (measured by ES) as
412 the constant weight strategy with weight p . The annualized alpha for this value of p is then

$$\alpha^p = \frac{\log(E[W_T^{opt,p}]) - \log(E[W_T^p])}{T}. \quad (8.3)$$

413 **Remark 8.1** (Optimal Efficient Frontier). *In practice, we compute the efficient frontier function*
414 *$F(ES_\beta^{opt})$ at a finite number of points, and approximate the efficient frontier function $F(\cdot)$ by linear*
415 *interpolation.*

416 9 Base Case: Synthetic Market

417 We compute and store the control determined by solving Problem 6.3 in the synthetic market using
418 the parameters from Table 7.1 for the investment scenario given in Table 7.2. We then use the

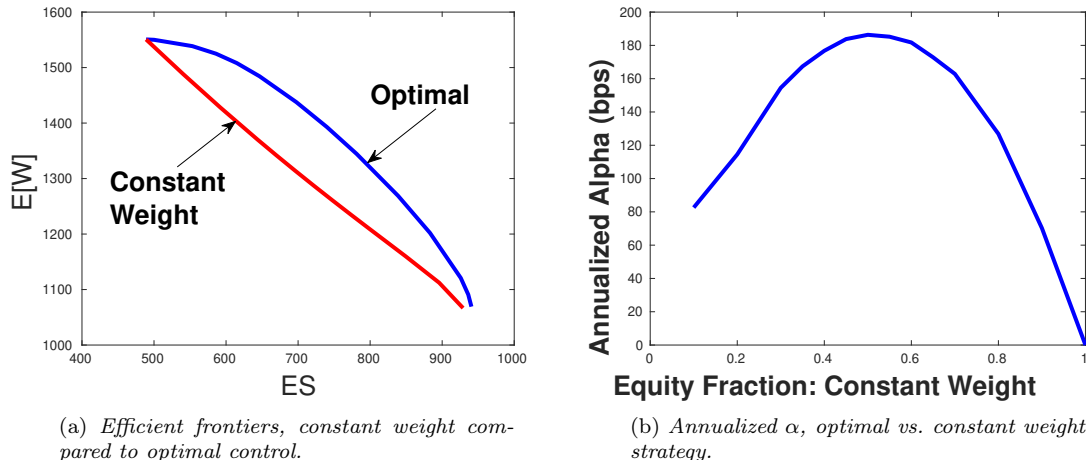


FIGURE 9.1: Scenario from Table 7.2, synthetic market. Optimal strategy determined by solving Problem 6.3 in the synthetic market, with parameters in Table 7.1. Control stored and then used to compute the final results with 2.56×10^6 Monte Carlo simulations.

419 stored control in Monte Carlo simulations to generate summary statistics. Figure 9.1(a) shows the
 420 EW-ES frontiers for the optimal strategy (6.3) and for the constant weight strategy.¹⁴ as a function
 421 of EW. Figure 9.1(b) shows the annualized alpha compared with the benchmark constant weight
 422 strategy, based on equation (8.3). The annualized alpha reaches a maximum of about 180 bps, when
 423 compared to a benchmark 60:40 stock bond portfolio.

424 Figure 9.2 shows the probability density of the internal rate of return for the optimal strategy in
 425 the synthetic market, for $\kappa = 1.0$. We also specify $W^* = 788$, which results in an ES approximately
 426 equal to that of a constant weight strategy with $p = 0.6$. Note the rapid decrease in the density
 427 near the 5th percentile and the long right tail. We can see that this density protects the downside
 428 (in terms of ES) and maximizes EW through the right skew.

429 Figure 9.3 compares the cumulative distribution functions (CDFs) for the optimal EW-ES strat-
 430 egy ($\kappa = 1.0$ and $W^* = 786$) and a constant weight strategy with $p = 0.6$. Both strategies have
 431 approximately the same ES(5%). The rapid decrease in the CDF for the optimal EW-ES strategy
 432 (near $W = 800$) results in the same tail risk as for the constant proportion strategy. The EW-ES
 433 policy then gives up some performance between final wealth values in the range $[800, 1260]$. However,
 434 the EW-ES strategy then gains in performance for $W_T > 1260$. This results in a larger expected
 435 final wealth value for the same tail risk. Note that there is no magic bullet in terms of strategies.
 436 If we constrain both strategies to have same left tail risk, then the EW-ES policy gives up some
 437 performance in the probability ranges from $[0.05, 0.55]$, in order to generate superior performance
 438 in the upper 45% of the outcomes. In other words, ignoring the left tail behavior (which is roughly
 439 the same), then the EW-ES strategy has slightly worse performance in 50% of the outcomes, which
 440 is counterbalanced by a large outperformance in 45% of the outcomes. This is essentially the oppo-
 441 site strategy compared to the multi-period pre-commitment Sharpe ratio maximizing (or quadratic
 442 shortfall) policy (Forsyth and Vetzal, 2017a;b; 2019). To emphasize this, Figure 9.4 provides an-
 443 other comparison of the constant weight (panel (a)) and EW-ES strategies (panel (b)), showing the

¹⁴Detailed tables containing the results used to generate Figure 9.1 are provided in Appendix E. Note that here expected terminal wealth as a function of ES is downward-sloping because higher ES represents lower risk. This is in contrast to cases like Figure 2.1(a) where risk (measured by standard deviation) was increasing along the horizontal axis.

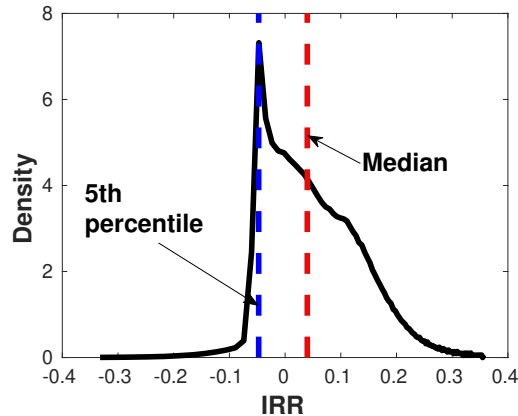


FIGURE 9.2: *Density of internal rate of return (IRR). Scenario from Table 7.2, synthetic market. Optimal strategy determined by solving Problem 6.3 with $\kappa = 1.0$ and $W^* = 788$ in the synthetic market, with parameters in Table 7.1. Control stored and then used to compute the final results with 6.4×10^5 Monte Carlo simulations. The IRR has a mean of .0724 and a median of .0396.*

444 densities of real wealth over time. Both strategies have approximately the same ES, but the EW-ES
 445 strategy has a large right skew. This is in stark contrast to the large left skew seen for the MV
 446 Optimal and Clipped MV Optimal strategies in Figure 2.3.

447 Figure 9.5 shows the percentiles of the fraction invested in stocks over time and the percentiles of
 448 total wealth for the EW-ES strategy. The median fraction invested in stocks is quite high, between
 449 .80 – .90, but there is a large gap between the median and 5th percentile, indicating that the strategy
 450 reacts very strongly to decreasing wealth, as shown in Figure 9.6 which provides a heatmap of the
 451 optimal controls. Initially, with $W_0 = 1000$ at $t = 0$ the equity weight is about 0.85. If the portfolio
 452 does well, the fraction in stocks remains high. However, if the portfolio performs poorly, the fraction
 453 in stocks is rapidly reduced. Further poor returns will result in a large fraction in bonds (in the
 454 blue zone of the heatmap) so as to protect the ES. Conversely, if stocks do well, the strategy will
 455 increase the allocation to stocks. Hence this is a momentum-type policy. However, if the portfolio
 456 suffers a very large sudden loss (basically jumping down through the blue zone in Figure 9.6), the
 457 strategy will once again increase the stock position. This can be seen as a last ditch attempt to
 458 recover, by taking a large equity position and hoping for strong returns. Similar behavior happens
 459 in the case of very poor investment returns for the MV Optimal strategy, as seen in Figure 2.2. On
 460 the whole, the momentum type of strategy shown in Figure 9.6 displays a much more varied pattern
 461 across both real wealth and time compared to the contrarian MV Optimal strategy in Figure 2.2.

462 10 Historical market

463 We next present historical market results. Recall that the procedure used here is to determine the
 464 optimal controls based on an assumed parametric model (in this case the double exponential jump
 465 diffusion processes (4.3) and (4.4)), and then apply the controls to resampled historical return data
 466 as described above in Section 2.1.

467 Figure 10.1 shows the efficient EW-ES frontiers and the apparent alpha for the bootstrapped
 468 historical market. The results are shown for various expected blocksizes (Blk) in years.¹⁵ We

¹⁵Appendix F provides detailed tables of the results used to generate Figure 10.1. To save space, we only provide the results for the case with an expected blocksize of 5 years.

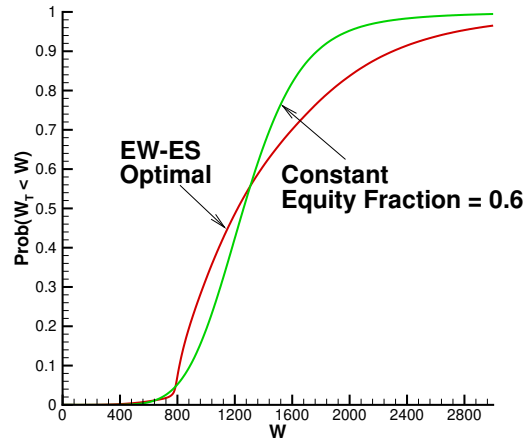


FIGURE 9.3: Cumulative distribution functions of terminal real wealth for the optimal EW-ES ($\kappa = 1.0, W^* = 786$) strategy compared to a constant weight strategy ($p = 0.6$). Both strategies have approximately the same $ES \in (696, 698)$. Scenario from Table 7.2, synthetic market. Optimal strategy determined by solving Problem 6.3 in the synthetic market, with parameters in Table 7.1. Control stored and then used to compute the final results with 2.56×10^6 Monte Carlo simulations.

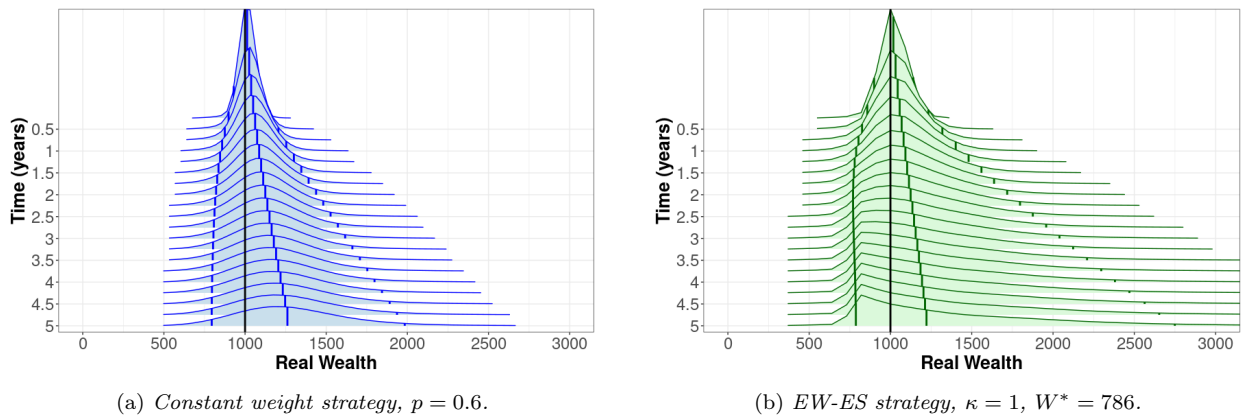
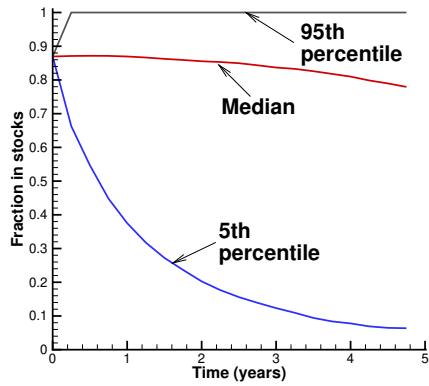
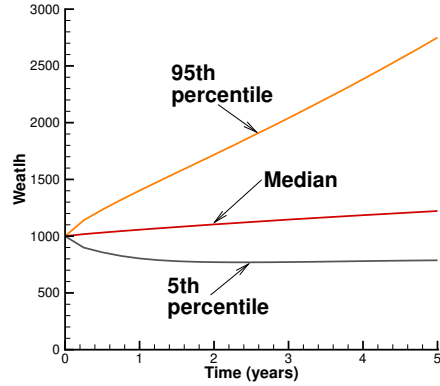


FIGURE 9.4: Densities of real wealth over time for constant weight ($p = 0.6$) and EW-ES ($\kappa = 1, W^* = 786$) strategies. Investment scenario from Table 7.2. 640,000 simulated synthetic market paths with quarterly rebalancing. Densities plotted quarterly. The black vertical line indicates the initial real wealth $W_0 = 1000$. The colored vertical lines in each density represent the 5th, 50th, and 95th percentiles of the distribution.



(a) Percentiles fraction in stocks.



(b) Percentiles wealth

FIGURE 9.5: Scenario in Table 7.2, synthetic market. Optimal strategy determined by solving Problem 6.3 in the synthetic market, parameters in Table 7.1. Control stored and then used to compute the final results with 6.4×10^5 Monte Carlo simulations. Parameters based on CRSP inflation adjusted data, 1926:1-2019:12. $\kappa = 1.0$.

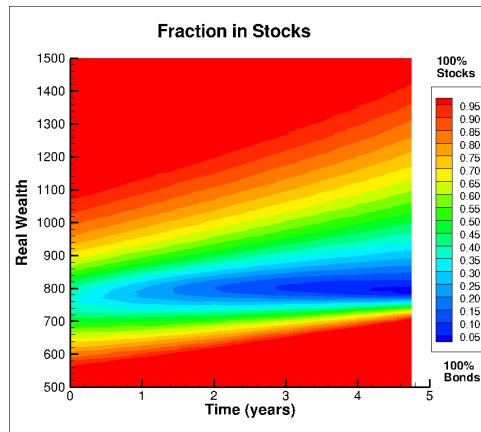


FIGURE 9.6: Heatmap of fraction in stocks. Scenario from Table 7.2. Optimal strategy determined by solving Problem 6.3 with $\kappa = 1.0$ and $W^* = 786$ in the synthetic market, with parameters in Table 7.1.

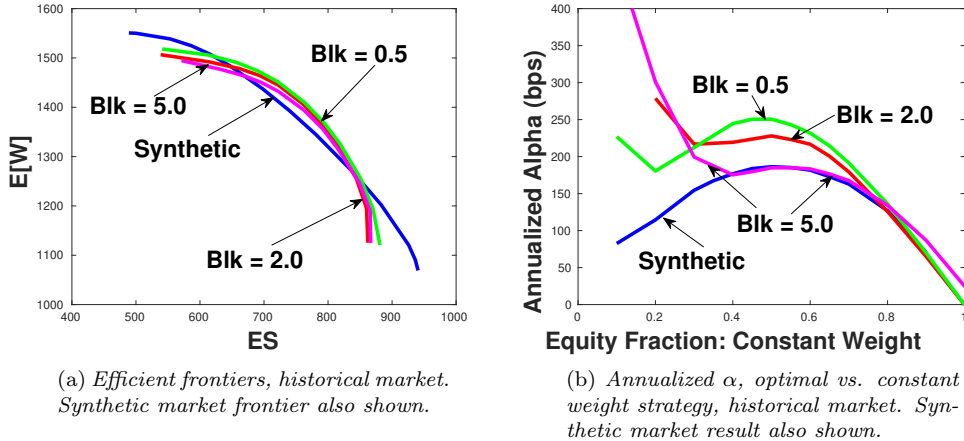


FIGURE 10.1: Optimal strategy determined by solving Problem 6.3 in the synthetic market, parameters in Table 7.1. Control stored and then tested in bootstrapped historical market. Non-Pareto points eliminated. Expected blocksize (Blk , years) used in the bootstrap resampling method also shown.

469 also show the synthetic market results as well for comparison. Figure 10.1(a) indicates that the
 470 control computed using the parametric model (synthetic market) performs quite well in the historical
 471 market, except for large values of ES. This indicates that the optimal controls are fairly robust to
 472 parametric model misspecification, over a wide range of interesting values of ES (i.e. ES in the range
 473 650 – 850). The results are also fairly insensitive to the choice of expected blocksize.

474 On the other hand, the apparent alpha based on the synthetic market control, tested in the
 475 historical market, is generally superior to the synthetic market controls tested in the synthetic
 476 market, especially for the interesting constant weight benchmark portfolios for p in the range 0.4 –
 477 0.6. However, while Figure 10.1(a) shows very little sensitivity to expected blocksize, Figure 10.1(b)
 478 is sensitive to blocksize. This is because the constant weight strategies are much more sensitive to the
 479 blocksize in the resampling algorithm compared to the EW-ES strategies, suggesting that constant
 480 weight strategies are less robust than EW-ES strategies.

481 The apparent alpha in Figure 10.1(b) is surprisingly large for small values of constant p for the
 482 benchmark portfolio. This results from the very poor performance of constant weight portfolios for
 483 small equity weights in the historical market.¹⁶ This can be verified by examining the case with
 484 $p = 0.0$ in Table F.2, which has an ES of about 764. In other words, short term T-bills have an
 485 expected loss in the worst 5% of cases of about 25% in real terms over five years. This is due to
 486 negative real short term interest rates in times of inflation.

487 Figure 10.2 depicts the evolution of the densities of real wealth over time in the historical market
 488 with an expected blocksize of 5 years, for both the constant weight ($p = 0.6$) and EW-ES strategies.
 489 The patterns observed here are quite similar to those seen above in Figure 9.4 in the synthetic
 490 market, although the results here are clearly not as smooth. The main features of the EW-ES
 491 strategy are preserved quite well in the historical market, as there is clear downside protection and
 492 a strong right skew indicating upside potential.

¹⁶Recall that we noted similar behavior for the Clipped MV Optimal strategy in Figure 2.4.

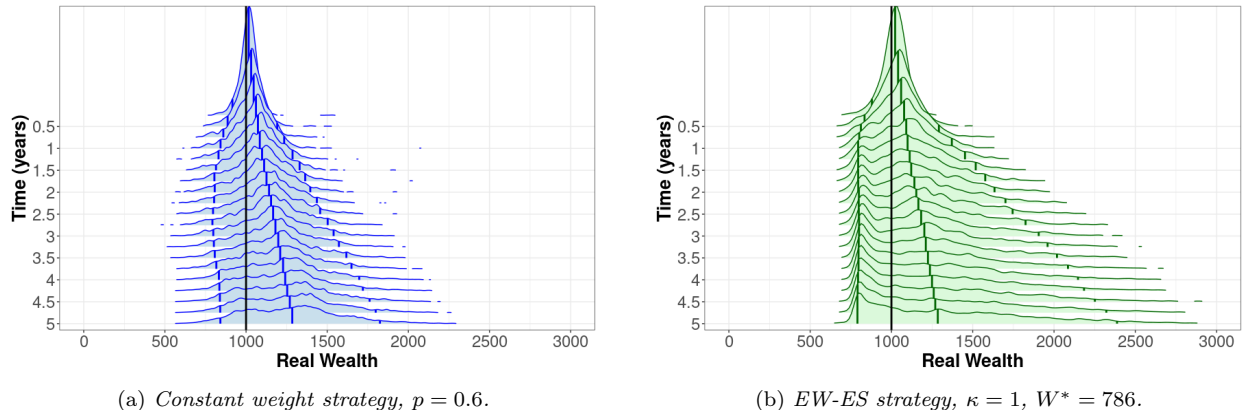


FIGURE 10.2: Densities of real wealth over time for constant weight ($p = 0.6$) and EW-ES ($\kappa = 1$, $W^* = 786$) strategies. Investment scenario from Table 7.2. 640,000 simulated historical market paths with expected blocksize 60 months and quarterly rebalancing. Densities plotted quarterly. The black vertical line indicates the initial real wealth $W_0 = 1000$. The colored vertical lines in each density represent the 5th, 50th, and 95th percentiles of the distribution.

493 11 Alternative Investment Scenarios

494 In this section we explore the effects of some departures from the base case assumptions presented
 495 in Table 7.2. We first study the rebalancing frequency and the potential use of leverage, and then
 496 turn to a shorter investment horizon. We concentrate here exclusively on the synthetic market.

497 11.1 Rebalancing Frequency and Leverage

498 Figure 11.1(a) shows the effect of changing the rebalancing frequency on the efficient frontiers (op-
 499 timal strategy, synthetic market). There is very little discernable effect of changing the rebalancing
 500 frequency from one month to six months.

501 Recall from Appendix A that continuous trading in the stock and bond with no leverage can
 502 replicate a covered call strategy. Since it appears from Figure 11.1(a) that the effect of the rebal-
 503 ancing frequency is small, this suggests that our discretely rebalanced portfolio can approximate a
 504 covered call strategy.

505 However, there may be other strategies which use options that allow the investor to use leverage
 506 with limited downside. Formally, these other option strategies would require continuous trading.
 507 However, we can approximate the effect of other strategies which include options by allowing the
 508 use of leverage.

509 Figure 11.1(b) shows the results for allowing leverage, both with and without a borrowing
 510 spread.¹⁷ For values of $ES > 750$, which is arguably the region of interest, the gain in using leverage
 511 is quite small. Figure 11.1(b) suggests that allowing the use of leverage is not very important for
 512 such values of ES . Hence there is no particular advantage to taking direct positions in options as
 513 compared to dynamic trading, unless the value of ES considered is quite small (i.e. the investor
 514 wants a very risky strategy).

¹⁷We enforce the constraint that trading ceases if insolvency occurs, and debt accumulates at the borrowing rate. However, the probability of this occurring over five years is very small.

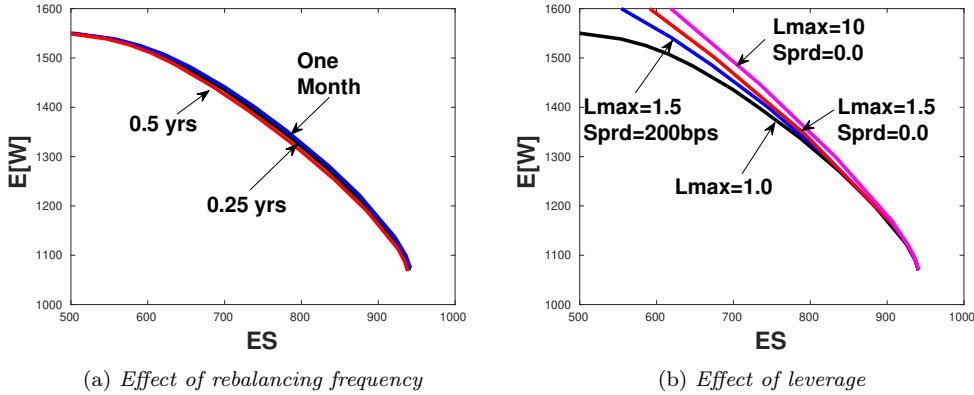


FIGURE 11.1: Synthetic market, optimal strategy, effect of rebalancing frequency and use of leverage. L_{\max} is the maximum value of p allowed. Optimal strategy determined by solving Problem 6.3 in the synthetic market, parameters in Table 7.1.

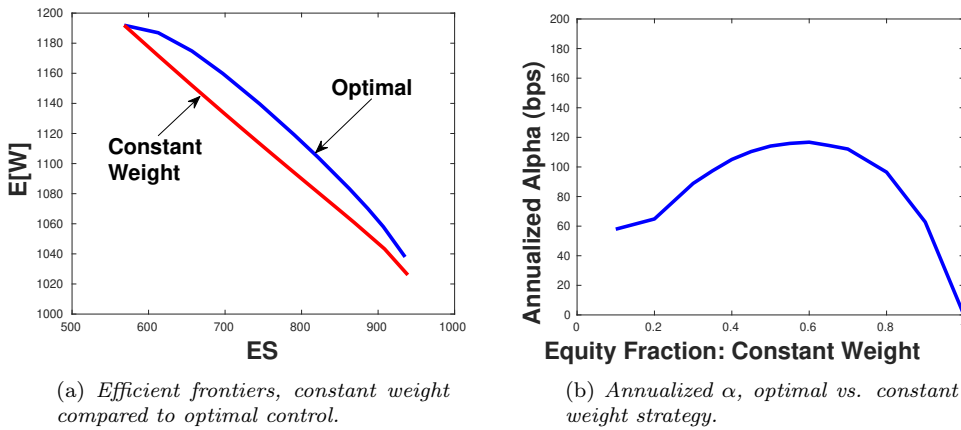


FIGURE 11.2: Scenario in Table 7.2, synthetic market. Optimal strategy determined by solving Problem 6.3 in the synthetic market, parameters in Table 7.1, with the exception that $T = 2.0$ years, and the portfolio is rebalanced monthly. Control stored and then used to compute the final results with 6.4×10^5 Monte Carlo simulations.

515 11.2 Two Year Time Horizon

516 It is also interesting to examine the effect of a shorter investment horizon. Up to now, we have been
 517 using $T = 5.0$ years. Figure 11.2 shows the results for the efficient EW-ES frontier and the apparent
 518 alpha for $T = 2.0$ years in the synthetic market with monthly rebalancing. It is interesting to see
 519 that even for this comparatively short time period, the apparent annualized alpha is roughly 120
 520 bps, compared to a constant weight strategy with $p = 0.6$. This compares with a maximum alpha
 521 of about 180 bps for the $T = 5$ years case.

522 Figure 11.3 shows the heatmap of the optimal controls (fraction in stocks) for the $T = 2$ years
 523 case with $\kappa = 2.25$. In contrast to the 5-year horizon case in Figure 9.6, here it can be seen that if
 524 stocks drop in value very early on, the optimal strategy is to quickly shift out of stocks into bonds.
 525 The optimal strategy ($T = 2$ years) is to heavily invest in bonds when the total wealth approaches
 526 $W^* = 828$.

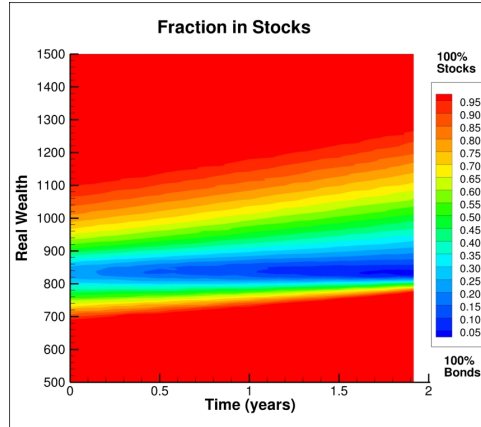


FIGURE 11.3: Heat map of fraction in stocks, scenario in Table 7.2, parameters from Table 7.1. Here $T = 2.0$ years, monthly rebalancing $\kappa = 2.25$, $W^* = 828$, $ES(5\%) = 745$, $E[W_T] = 1140$. Compare with Figure 9.6 ($T = 5$ years).

527 12 Discussion

528 Sharpe ratio maximizing strategies exploit the symmetry of the standard deviation risk measure by
 529 selling off large gains. In some circumstances, such as saving for retirement in a DC savings account,
 530 multi-period Sharpe ratio maximization can in fact be useful. However, this is due to the fact that
 531 multi-period Sharpe ratio maximizing strategies are equivalent to an induced time consistent target
 532 based quadratic shortfall minimization (Vigna, 2014). It is this property, rather than Sharpe ratio
 533 maximization *per se*, which is desirable for DC plan investments.

534 In order to align the objective function more precisely with an investor’s intuitive concept of risk,
 535 we propose using an asymmetric risk measure that is based on expected shortfall (ES). Although this
 536 strategy is formally a pre-commitment policy, we argue that the lack of time consistency in this case
 537 does not cause conceptual difficulties. We can think of this strategy as part of a packaged product
 538 sold to a retail customer who does not trade in the underlying securities during the lifetime of the
 539 contract. This packaged product is essentially a *black box* to the retail customer, who evaluates
 540 success or failure of this policy based on the initial investment and final value.

541 The optimal policy is based on determining the expected wealth, expected shortfall (EW-ES)
 542 frontiers. This strategy cuts off the left tail of the distribution (protecting worst case wealth out-
 543 comes), with a skewed right tail, which maximizes EW. This strategy might be regarded as having
 544 some of the features of value investing, where preservation of capital is given the highest priority.
 545 However, in this case, capital is preserved by dynamic trading rather than stock picking.

546 Note that Sharpe ratio maximizing strategies have a contrarian flavor. They can be summarized
 547 as “buy stocks and sell bonds when stocks go down, sell stocks and buy bonds when stocks go up.”
 548 The EW-ES policy is essentially the opposite, sell stocks and buy bonds when stocks go down; buy
 549 stocks and sell bonds when stocks go up: “cut your losses, ride your gains”. This is essentially a
 550 momentum type of strategy.

551 A negative feature with this EW-ES strategy (which it shares with the constant proportion
 552 portfolio insurance strategy (CPPI) (Black and Jones, 1987)) is the possibility of cashing out, i.e.
 553 if stocks drop early in the investment process, the portfolio will move to largely bond holdings,
 554 with little possibility of recovery. This strategy will be particularly ineffective in the case of a large
 555 market drop, followed by a rapid recovery, such as the recent pandemic market crash and recovery.
 556 This is, however, a very unusual return sequence based on U.S. market history.

557 **13 Conclusion**

558 We have reviewed the known results concerning dynamic strategies which maximize the Sharpe
559 ratio. These strategies essentially reduce risk by selling off the right tail of the distribution. While
560 this approach may be desirable in some circumstances (e.g. when saving for retirement where a
561 target-based strategy can be used to generate cash flows to replace employment income (Forsyth
562 and Vetzal, 2019)), this may not be a suitable approach for all investors.

563 Denoting the expected terminal wealth by EW, and the expected shortfall by ES (ES is the mean
564 of the worst β fraction of outcomes), we propose an objective function based on EW-ES criteria.
565 Measuring risk by ES (expected shortfall) fundamentally means that the investor is concerned with
566 the left tail risk. This amounts to preserving a desired minimum value of terminal wealth, with high
567 probability. We determine the optimal EW-ES dynamic trading strategy using optimal stochastic
568 control techniques, based on a parametric model for stock and bond processes, fit to historical data.
569 We impose realistic constraints on the trading strategy: no-leverage, no-shorting, and infrequent
570 rebalancing.

571 We define the alpha of this investment strategy relative to a benchmark by using ES as the
572 measure of risk. We focus on medium-term investments (i.e. 2-5 years), where wealth preservation
573 can be regarded as of high importance. Compared to a 60:40 stock-bond constant weight strategy,
574 the optimal EW-ES policy gives an annualized alpha of about 180 bps over a 5-year investment
575 horizon.

576 We emphasize again that optimal EW-ES strategies are fundamentally different compared to
577 Sharpe ratio maximizing strategies. Optimal Sharpe ratio strategies are contrarian: increase the
578 weight in stocks when stocks do poorly and decrease the weight in stocks when stocks do well.
579 EW-ES optimal strategies do the opposite: decrease the weight in stocks when stocks perform poorly,
580 increase the weight in stocks when stocks do well. This policy protects the left tail, while taking
581 advantage of the large possible gains emanating from the right tail of the distribution. Finally, it is
582 worth noting that bootstrap resampling tests using historical data show that the optimal EW-ES
583 policy is fairly robust to parametric model misspecification.

584 **14 Acknowledgment**

585 Forsyth's work was supported by the Natural Sciences and Engineering Research Council of Canada
586 (NSERC) grant RGPIN-2017-03760.

587 **15 Disclosure**

588 The authors report there are no competing interests to declare.

589 **Appendices**

590 **A Replication of Covered Call and Cash-Secured Put Writing**

591 This appendix outlines the assumptions required to ensure that dynamic trading in stocks and risk-
592 less bonds can replicate covered call and cash-secured put writing, which are two popular approaches
593 to generating apparent alpha (Lhabitant, 2000; Goetzmann et al., 2002; Ungar and Moran, 2009).

594 **Assumption A.1.** Let $V(S,t)$ be the price of a call or put option, with S being the unit price of
 595 the stock.¹⁸ We make the following assumptions:

596 (i) Trading in the stock with price $S(t)$ and the riskless bond $B(t)$ occur continuously, with no
 597 market frictions.

598 (ii) Call and put option prices are convex.

599 (iii) Call and put options can be perfectly replicated by the portfolio of $\alpha(S,t)$ units stock and an
 600 amount $B(S,t)$ in the riskless bond which pays an interest rate of r , so that the total value of
 601 the replicating portfolio is

$$V(S,t) = \alpha S + B \quad (\text{A.1})$$

602 with $\alpha = V_S$. At points where V_S does not exist (which can only occur at a countable number
 603 of points), we take the appropriate left or right limits.

(iv) V_S satisfies the bounds

$$\begin{aligned} 0 &\leq V_S \leq 1 && \text{Call} \\ -1 &\leq V_S \leq 0 && \text{Put} \end{aligned}$$

604 (v) The value of a call option at $S = 0$ is zero. The value of a European put at $S = 0$ is $Ke^{-r(T-t)}$,
 605 where K is the strike, and T is the expiry time. The value of an American put at $S = 0$ is K .

606 Some discussion concerning the conditions under which assumptions (i)-(iv) hold is given in
 607 Bergman et al. (1996). Suffice to say, all these assumptions are met in a Black-Scholes market, as
 608 used for the background example in Section 2.

609 **Proposition A.1.** Under Assumptions A.1, covered call writing and cash-secured put writing can
 610 be replicated by a portfolio consisting of the underlying asset and riskless bond with non-negative
 611 amounts in both stock and bond, i.e. the portfolio satisfies the no-shorting, no leverage condition
 612 $0 \leq p \leq 1$ where p is the fraction of the portfolio wealth held in the risky asset.

613 *Proof.* We consider first the case of a stock which does not pay dividends.

614 (a) **Covered Call:** Consider a covered call long one unit of stock, short one call option and long
 615 the option premium. By definition $S \geq 0$. At $t = 0$, the covered call portfolio Π^{cc} is

$$\begin{aligned} \Pi^{cc}(S,0) &= S - \overbrace{V(S,0)}^{\text{short call}} + \overbrace{V_0}^{\text{cash premium}} \\ V_0 &= V(S,0) . \end{aligned} \quad (\text{A.2})$$

Replace $V(S,0)$ by the replicating portfolio

$$\begin{aligned} V(S,0) &= \alpha(S,0)S + B(S,0) \\ \alpha(S,0) &= V_S(S,0), \end{aligned} \quad (\text{A.3})$$

616 where the amount in the riskless bond is

$$B(S,0) = V(S,0) - V_S(S,0)S. \quad (\text{A.4})$$

¹⁸With an abuse of notation, in this appendix S and B are the unit prices of the stock and bond respectively, not the amounts invested in them.

617 Then equation (A.2) becomes

$$\Pi^{cc}(S,0) = S - (\alpha(S,0)S + B(S,0)) + V_0 . \quad (\text{A.5})$$

In general for $t > 0$ we have

$$\Pi^{cc}(S,t) = S - \alpha(S,t)S - B(S,t) + V_0 e^{rt} \quad (\text{A.6})$$

$$B(S,t) = V(S,t) - \alpha(S,t)S , \quad (\text{A.7})$$

618 where r is the continuously compounded risk-free rate, and so

$$\Pi^{cc}(S,t) = \overbrace{S(1-\alpha)}^{\text{stock position}} + \overbrace{V_0 e^{rt} - B(S,t)}^{\text{cash}} . \quad (\text{A.8})$$

619 Consider the line in the (V,S) plane

$$\alpha(S^*,t)S + C , \quad (\text{A.9})$$

620 where the constant C is determined from

$$\alpha(S^*,t)S^* + C = V(S^*,t) . \quad (\text{A.10})$$

621 The line (A.9) is then tangent to the option value $V(S,t)$ at $S = S^*$. Since V is convex, it lies at or
 622 above its tangent line everywhere, including at $S = 0$ where $V(0,t) = 0$, which implies that $C \leq 0$.
 623 Since this is true for any S^* , then $(-B(S,t)) = \alpha(S,t)S - V(S,t) \geq 0$. For a call $0 \leq \alpha \leq 1$, so from
 624 equation (A.8) the stock position is also non-negative.

625 (b) **Cash-Secured Put:** Now consider writing a cash-secured put with strike K . If the put
 626 is European-style, the writer is long Ke^{-rT} in cash, short one put option, and long the option
 627 premium. By put-call parity and the results from (a), the cash-secured put also has non-negative
 628 positions in both the cash and stock.

If the put is American-style, the writer deposits K with the broker. At $t = 0$, the cash-secured
 put portfolio $\Pi^{cp}(S,t)$ is

$$\Pi^{cp}(S,0) = K - \overbrace{V(S,0)}^{\text{short put}} + \overbrace{V_0}^{\text{cash premium}} \\ V_0 = V(S,0) . \quad (\text{A.11})$$

Replace $V(S,0)$ by the replicating portfolio

$$V(S,0) = \alpha(S,0)S + B(S,0) \\ \alpha(S,0) = V_S(S,0) , \quad (\text{A.12})$$

629 where the amount in the riskless bond is

$$B(S,0) = V(S,0) - V_S(S,0)S . \quad (\text{A.13})$$

630 Then equation (A.11) becomes

$$\Pi^{cp}(S,0) = K - (\alpha(S,0)S + B(S,0)) + V_0 \quad (\text{A.14})$$

In general, for $t > 0$ we have

$$\Pi^{cp} = Ke^{rt} - \alpha(S,t)S - B(S,t) + V_0 e^{rt} \quad (\text{A.15})$$

$$B(S,t) = V(S,t) - \alpha(S,t)S , \quad (\text{A.16})$$

631 OR

$$\Pi^{cp} = \overbrace{-\alpha S}^{\text{stock position}} + \overbrace{V_0 e^{rt} + K e^{rt} - B(S,t)}^{\text{cash}} . \quad (\text{A.17})$$

632 Consider the line in the (V,S) plane

$$\alpha(S^*,t)S + C , \quad (\text{A.18})$$

633 where the constant C is determined by

$$\alpha(S^*,t)S^* + C = V(S^*,t) , \quad (\text{A.19})$$

634 so that (A.18) is tangent to $V(S,t)$ at $S = S^*$.

635 Since V is convex, it lies at or above its tangent line everywhere, including at $S = 0$ where
 636 $V(0,t) = K$, which implies that $C \leq K$. Hence $V(S^*,t) - \alpha(S^*,t)S^* = B(S^*,t) = C \leq K$. This is
 637 true for any S^* , so that $(K e^{rt} - B(S,t)) \geq 0$. Since $-1 \leq \alpha \leq 0$ for a put, the stock position is
 638 non-negative.

639 (c) **Dividends:** Now consider the case of a covered call written on a stock which pays a non-
 640 proportional dividend of $\min(D,S)$ at $t = t_d$. Let t_d^- be the instant before t_d . Then

$$\Pi^{cc}(S^-,t_d^-) = \overbrace{S^-(1 - \alpha^-)}^{\text{stock position}} - \overbrace{B(S^-,t_d^-) + V_0 e^{rt}}^{\text{cash}} , \quad (\text{A.20})$$

641 where by the arguments in (a) above the stock position is non-negative and $-B(S^-,t_d^-) =$
 642 $-B^- \geq 0$. At t_d^+ , after the dividend is paid, the new stock and cash positions are

$$\begin{aligned} (\text{stock position})^+ &= (S^- - \min(S^-,D))(1 - \alpha^-) \\ (\text{cash position})^+ &= -B^- + \min(S^-,D)(1 - \alpha^-) \end{aligned} \quad (\text{A.21})$$

643 From (a) above, $(1 - \alpha^-) \geq 0$ and $-B^- \geq 0$, so both positions are nonnegative after the
 644 dividend is paid. After rebalancing the replicating portfolio after the dividend payment, the stock
 645 and bond positions remain non-negative.¹⁹ The cash-secured put case can also be proven using
 646 similar arguments. \square

647 B Induced Time Consistent Policy

648 Noting that the inner supremum in equation (6.4) is a continuous function of W^* , define

$$\mathcal{W}^*(s,b) = \arg \max_{W^*} \left\{ \sup_{\mathcal{P}_0 \in \mathcal{A}} \left\{ E_{\mathcal{P}_0}^{X_0^+, t_0^+} \left[W^* + \frac{1}{\beta} \min(W_T - W^*, 0) + \kappa W_T \middle| X(t_0^-) = (s,b) \right] \right\} \right\} . \quad (\text{B.1})$$

649 We refer the reader to Forsyth (2020a) for an extensive discussion concerning pre-commitment and
 650 time consistent ES strategies. We summarize the relevant results from that research here. Denote
 651 the investor's initial wealth at t_0 by W_0^- . Then we have the following result:

Proposition B.1 (Pre-commitment strategy equivalence to a time consistent policy for an alternative objective function). *The pre-commitment EW-ES strategy \mathcal{P}^* determined by solving $J(0, W_0, t_0^-)$*

¹⁹Since $V(S^-,t) = V(S^- - \min(D,S^-),t^+)$, then $V_S(S^-,t) = V_S(S^+,t^+)$ and we don't actually need to rebalance across the dividend date.

(with $\mathcal{W}^*(0, W_0^-)$ from equation (B.1)) is the time consistent strategy for the equivalent problem TCEQ (with fixed $\mathcal{W}^*(0, W_0^-)$), with value function $\tilde{J}(s, b, t)$ defined by

$$\text{TCEQ}_{t_n}(\kappa\beta) : \quad \tilde{J}(s, b, t_n^-) = \sup_{\mathcal{P}_n \in \mathcal{A}} \left\{ E_{\mathcal{P}_n}^{X_n^+, t_n^+} \left[\min(W_T - \mathcal{W}^*(0, W_0^-), 0) + (\kappa\beta)W_T \right. \right. \\ \left. \left. \left| X(t_n^-) = (s, b) \right. \right] \right\}. \quad (\text{B.2})$$

652 *Proof.* This follows similar steps as in Forsyth (2020a), proof of Proposition 6.2. \square

653 **Remark B.1** (An Implementable Strategy). *Given an initial level of wealth W_0^- at t_0 , the optimal*
 654 *control for the pre-commitment problem (6.2) is the same optimal control for the time consistent*
 655 *problem (TCEQ $_{t_n}(\kappa\beta)$) (B.2), $\forall t > 0$. Hence we can regard problem (TCEQ $_{t_n}(\kappa\beta)$) as the EW-*
 656 *ES induced time consistent strategy. The induced strategy is implementable, in the sense that the*
 657 *investor has no incentive to deviate from the strategy computed at time zero at later times (Forsyth,*
 658 *2020a).*

659 C Algorithm for EW-ES Strategy

660 We use the method described in Forsyth (2020a) to solve Problem 6.2. We give a brief description
 661 of this technique below. We write equation (6.4) as

$$J(s, b, t_0^-) = \sup_{W^*} V(s, b, 0^-), \quad (\text{C.1})$$

where the auxiliary function $V(s, b, t)$ is defined as

$$V(s, b, W^*, t_n^-) = \sup_{\mathcal{P}_n \in \mathcal{A}_n} \left\{ E_{\mathcal{P}_n}^{X_n^+, t_n^+} \left[W^* + \frac{1}{\beta} \min((W_T - W^*), 0) + \kappa W_T \left| X(t_n^-) = (s, b) \right. \right] \right\}. \quad (\text{C.2})$$

$$\text{subject to } \begin{cases} (S_t, B_t) \text{ follow processes (4.3) and (4.4); } t \notin \mathcal{T} \\ W_\ell^+ = S_\ell^- + B_\ell^-; X_\ell^+ = (S_\ell^+, B_\ell^+) \\ S_\ell^+ = p_\ell(\cdot)W_\ell^+; B_\ell^+ = (1 - p_\ell(\cdot))W_\ell^+ \\ p_\ell(\cdot) \in \mathcal{Z} \\ \ell = n, \dots, M; t_\ell \in \mathcal{T} \end{cases}. \quad (\text{C.3})$$

662 We have now decomposed the original problem (6.2) into two steps

- 663 • Given an initial cash value of W_0 , and a fixed value of W^* , we solve problem (C.2) to determine
 664 $V(0, W_0, W^*, 0^-)$.
- 665 • Then, we solve the original problem (6.2) by maximizing over W^*

$$J(0, W_0, 0^-) = \sup_{W^*} V(0, W_0, W^*, 0^-). \quad (\text{C.4})$$

666 **C.1 Solution of Problem C.2**

667 We solve Problem C.2 by dynamic programming. Set

$$V(s, b, W^*, T^+) = W^* + \frac{\min((s + b - W^*), 0)}{\beta} + \kappa(s + b). \quad (\text{C.5})$$

For $t \in (t_{M-1}^+, t_M^-)$, we solve the PIDE

$$\begin{aligned} V_t + \frac{(\sigma^s)^2 s^2}{2} V_{ss} + (\mu^s - \lambda_\xi^s \gamma_\xi^s) s V_s + \lambda_\xi^s \int_{-\infty}^{+\infty} V(e^y s, b, t) f^s(y) dy + \frac{(\sigma^b)^2 b^2}{2} V_{bb} \\ + (\mu^b + \mu_c^b \mathbf{1}_{\{b < 0\}} - \lambda_\xi^b \gamma_\xi^b) b V_b + \lambda_\xi^b \int_{-\infty}^{+\infty} V(s, e^y b, t) f^b(y) dy - (\lambda_\xi^s + \lambda_\xi^b) V + \rho_{sb} \sigma^s \sigma^b s b V_{sb} = 0. \end{aligned} \quad (\text{C.6})$$

668 At rebalancing time t_{M-1} , we determine the optimal control $p_{M-1}(w = s + b, W^*)$ from

$$p_{M-1}(w, W^*) = \arg \max_{p' \in \mathcal{Z}} V(wp', w(1 - p'), W^*, t_{M-1}^+), \quad (\text{C.7})$$

669 so that

$$V(s, b, W^*, t_{M-1}^-) = V(wp_{M-1}(w, W^*), w(1 - p_{M-1}(w, W^*)), t_{M-1}^+). \quad (\text{C.8})$$

670 Working backwards, we continue in this way until we reach t_0 .

671 **C.2 Numerical Techniques**

672 We localize the infinite domain to $(s, b) \in [s_{\min}, s_{\max}] \times [b_{\min}, b_{\max}]$, and discretize $[b_{\min}, b_{\max}]$ using
 673 an equally spaced $\log b$ grid with n_b nodes. Similarly, we discretize $[s_{\min}, s_{\max}]$ on an equally spaced
 674 $\log s$ grid with n_s nodes. For the case where we allow leverage, we also define a reflected grid with
 675 $b < 0$. We use the Fourier method in (Forsyth and Labahn, 2019) to solve PIDE (C.6). Localization
 676 errors are minimized using the domain extension method in (Forsyth and Labahn, 2019).

677 At rebalancing dates, we solve the optimization problem (C.7) by discretizing $p(\cdot)$ and using
 678 exhaustive search. Finally, the optimization problem (C.1) is solved using a one-dimensional opti-
 679 mization technique. Note that each evaluation of the objective function requires solution of problem
 680 (C.2) with a fixed value of W^* .

681 We compute and store the optimal controls from solving Problem 6.2 using the parametric model
 682 of the stock and bond processes. We then use the stored controls in Monte Carlo simulations to
 683 generate statistical results. As a robustness check, we also use the stored controls and simulate
 684 results using bootstrap resampling of historical data.

685 **D Convergence Test**

686 Table D.1 shows a detailed convergence test for the base case problem given in Table 7.2. As
 687 expected, we can see that the value function converges at a rate between first and second order.
 688 The ES and EW values, which are derived quantities, converge a bit more erratically. Note that
 689 there is good agreement between the algorithm in Section C and the Monte Carlo validation. We
 690 remind the reader that the controls (the fraction in stocks) are determined using the method in
 691 Section C. These controls are then used in the Monte Carlo simulations.

Algorithm in Section C				Monte Carlo	
Grid	ES (5%)	$E[W_T]$	Value Function	ES (5%)	$E[W_T]$
512×512	672.62	1457.68	2130.3	682.06	1450.78
1024×1024	695.15	1437.64	2132.8	698.66	1436.31
2048×2048	696.59	1437.95	2134.5	697.56	1437.73
4096×4096	698.41	1436.72	2135.1	698.68	1436.65

TABLE D.1: *Convergence test for scenario in Table 7.2 with parameters in Table 7.1. The Monte Carlo method used 2.56×10^6 simulations. $\kappa = 1.0, \alpha = .05$. Grid refers to the grid used in the Algorithm in Section C: $n_x \times n_b$, where n_x is the number of nodes in the log s direction and n_b is the number of nodes in the log b direction.*

692 E Detailed Efficient Frontiers: Synthetic Market

693 Tables E.1 and E.2 give the detailed results used to construct Figure 9.1(a).

κ	ES (5%)	$E[W_T]$	Median[W_T]
0.1	940.60	1069.19	1051.51
0.25	936.23	1090.89	1056.85
0.4	925.85	1120.77	1063.53
0.6	883.094	1202.04	1083.39
0.7	838.84	1268.85	1107.31
0.8	781.29	1344.45	1146.52
0.9	739.88	1392.98	1179.12
1.0	697.56	1437.73	1222.12
1.2	646.41	1484.39	1291.43
1.5	614.92	1508.10	1347.72
2.0	586.16	1524.96	1381.78
3.0	553.23	1538.65	1399.09
10.0	500.08	1550.05	1405.02
∞	489.00	1550.71	1405.15

TABLE E.1: *Synthetic market results for optimal strategies, assuming the scenario given in Table 7.2. Control determined by solving Problem 6.3. Stock index: real capitalization weighted CRSP stocks; bond index: 30-day T-bills. Parameters from Table 7.1. Units: thousands of dollars. Statistics based on 2.56×10^6 Monte Carlo simulation runs.*

694 F Detailed Efficient Frontiers: Historical Market

695 Tables F.1-F.2 give the detailed results used to generate Figure 10.1. We show only the case where
696 the expected blocksize is 5 years.

Constant weight p	ES (5%)	$E[W_T]$	$Median[W_T]$
0.0	917.26	1022.76	1023.45
0.1	929.03	1066.65	1063.48
.20	895.80	1112.34	1103.31
.30	849.32	1159.87	1143.32
.35	824.46	1184.35	1163.24
.40	799.09	1209.33	1183.09
.45	773.44	1234.81	1202.82
.50	747.62	1260.79	1222.33
.55	721.71	1287.29	1241.68
.60	695.77	1314.33	1260.89
.65	669.84	1341.90	1279.88
.70	643.93	1370.02	1298.64
.80	592.19	1427.94	1335.30
.90	540.58	1488.19	1370.95
1.0	489.00	1550.71	1405.15

TABLE E.2: *Synthetic market results for constant weight strategies. Stock index: real capitalization weighted CRSP stocks; bond index: 30-day T-bills. Parameters from Table 7.1. Units: thousands of dollars. Statistics based on 2.56×10^6 Monte Carlo simulation runs.*

κ	ES (5%)	$E[W_T]$	$Median[W_T]$
0.1	846.10	1085.38	1052.49
0.25	855.16	1101.88	1062.07
0.4	866.53	1124.61	1075.61
0.6	865.83	1189.97	1115.54
0.7	848.92	1247.14	1150.09
0.8	816.59	1313.73	1198.20
0.9	791.41	1356.67	1237.18
1.0	762.13	1394.46	1284.53
1.2	722.44	1432.22	1357.37
1.5	695.87	1450.28	1410.98
2.0	669.71	1463.51	1437.64
3.0	631.84	1476.97	1448.58
10.0	571.11	1494.62	1452.69

TABLE F.1: *Historical market results for optimal strategies, assuming the scenario given in Table 7.2. Control determined by solving Problem 6.3. Stock index: real capitalization weighted CRSP stocks; bond index: 30-day T-bills. Scenario Table 7.1. Units: thousands of dollars. Statistics based on 10^6 bootstrapped simulations. Expected blocksize of 5 years.*

697 References

- 698 Bauerle, N. and S. Grether (2015). Complete markets do not allow free cash flow streams. *Mathe-*
699 *matical Methods of Operations Research* 81, 137–146.
- 700 Bergman, Y. Z., B. D. Grundy, and Z. Wiener (1996). General properties of option prices. *Journal*
701 *of Finance* 51, 1573–1610.
- 702 Bernard, C. and S. Vanduffel (2014). Mean-variance optimal portfolios in the presence of a bench-

Constant weight p	ES (5%)	$E[W_T]$	$Median[W_T]$
0.0	763.98	1029.82	1023.02
0.1	804.41	1070.73	1061.82
0.2	833.61	1112.67	1109.03
0.3	841.16	1155.72	1152.42
0.4	826.08	1199.95	1197.04
0.45	811.92	1222.55	1217.27
0.5	795.27	1245.46	1238.77
0.55	776.71	1268.71	1261.33
.60	756.67	1292.31	1284.25
.65	735.46	1316.27	1306.29
.70	712.98	1340.60	1326.66
.80	664.99	1390.41	1371.08
.90	614.04	1441.81	1411.06
1.0	560.63	1494.91	1452.69

TABLE F.2: Historical market results for constant weight strategies, assuming the scenario given in Table 7.2. Stock index: real capitalization weighted CRSP stocks; bond index: 30-day T-bills. Scenario in Table 7.1. Units: thousands of dollars. Statistics based on 10^6 bootstrapped simulations. Expected blocksize of 5 years.

703 mark with applications to fraud detection. *European Journal of Operational Research* 234, 469–
704 480.

705 Black, F. and R. W. Jones (1987). Simplifying portfolio insurance. *The Journal of Portfolio*
706 *Management* 14:1, 48–51.

707 Cont, R. and C. Mancini (2011). Nonparametric tests for pathwise properties of semimartingales.
708 *Bernoulli* 17, 781–813.

709 Cui, X., D. Li, S. Wang, and S. Zhu (2012). Better than dynamic mean-variance: time inconsistency
710 and free cash flow stream. *Mathematical Finance* 22, 346–378.

711 Dang, D.-M. and P. A. Forsyth (2016). Better than pre-commitment mean-variance portfolio al-
712 location strategies: a semi-self-financing Hamilton-Jacobi-Bellman equation approach. *European*
713 *Journal of Operational Research* 250, 827–841.

714 Dichtl, H., W. Drobetz, and M. Wambach (2016). Testing rebalancing strategies for stock-bond
715 portfolios across different asset allocations. *Applied Economics* 48, 772–788.

716 Dybvig, P. H. and J. E. Ingersoll (1982). Mean-variance theory in complete markets. *Journal of*
717 *Business* 55:2, 233–251.

718 Forsyth, P. and G. Labahn (2019). ϵ -Monotone Fourier methods for optimal stochastic control in
719 finance. *Journal of Computational Finance* 22:4, 25–71.

720 Forsyth, P. A. (2020a). Multi-period mean CVAR asset allocation: Is it advantageous to be time
721 consistent? *SIAM Journal on Financial Mathematics* 11:2, 358–384.

722 Forsyth, P. A. (2020b). Optimal dynamic asset allocation for DC plan accumulation/decumulation:
723 Ambition-CVAR. *Insurance: Mathematics and Economics* 93, 230–245.

- 724 Forsyth, P. A. and K. R. Vetzal (2017a). Dynamic mean variance asset allocation: Tests for
725 robustness. *International Journal of Financial Engineering* 4, 1750021:1–1750021:37. DOI:
726 10.1142/S2424786317500219.
- 727 Forsyth, P. A. and K. R. Vetzal (2017b). Robust asset allocation for long-term target-based invest-
728 ing. *International Journal of Theoretical and Applied Finance* 20:3. Article 1750017/1-32.
- 729 Forsyth, P. A. and K. R. Vetzal (2019). Optimal asset allocation for retirement savings: deterministic
730 vs. time consistent adaptive strategies. *Applied Mathematical Finance* 26:1, 1–37.
- 731 Goetzmann, W., J. E. Ingersoll, M. Spiegel, and I. Welch (2002). Sharpening Sharpe ratios. NBER
732 working paper, 9116.
- 733 Kou, S. G. (2002). A jump-diffusion model for option pricing. *Management Science* 48, 1086–1101.
- 734 Kou, S. G. and H. Wang (2004). Option pricing under a double exponential jump diffusion model.
735 *Management Science* 50, 1178–1192.
- 736 Lhabitant, F.-S. (2000). Derivatives in portfolio management: why beating the market is easy.
737 Working paper, EDHEC Business School.
- 738 Li, D. and W.-L. Ng (2000). Optimal dynamic portfolio selection: multiperiod mean-variance
739 formulation. *Mathematical Finance* 10, 387–406.
- 740 Lin, Y., R. MacMinn, and R. Tian (2015). De-risking defined benefit plans. *Insurance: Mathematics*
741 *and Economics* 63, 52–65.
- 742 Ma, K. and P. A. Forsyth (2016). Numerical solution of the Hamilton-Jacobi-Bellman formula-
743 tion for continuous time mean variance asset allocation under stochastic volatility. *Journal of*
744 *Computational Finance* 20(1), 1–37.
- 745 MacMinn, R., P. Brockett, J. Wang, Y. Lin, and R. Tian (2014). The securitization of longevity risk
746 and its implications for retirement security. In O. S. Mitchell, R. Maurer, and P. B. Hammond
747 (Eds.), *Recreating Sustainable Retirement*, pp. 134–160. Oxford: Oxford University Press.
- 748 Mancini, C. (2009). Non-parametric threshold estimation models with stochastic diffusion coefficient
749 and jumps. *Scandinavian Journal of Statistics* 36, 270–296.
- 750 Menoncin, F. and E. Vigna (2017). Mean-variance target based optimisation for defined contribution
751 pension schemes in a stochastic framework. *Insurance: Mathematics and Economics* 76, 172–184.
- 752 Moussawi, R., K. Shen, and R. Velthuis (2022). The role of taxes in the rise of ETFs. SSRN
753 3744519.
- 754 Patton, A., D. Politis, and H. White (2009). Correction to: automatic block-length selection for
755 the dependent bootstrap. *Econometric Reviews* 28, 372–375.
- 756 Politis, D. and J. Romano (1994). The stationary bootstrap. *Journal of the American Statistical*
757 *Association* 89, 1303–1313.
- 758 Politis, D. and H. White (2004). Automatic block-length selection for the dependent bootstrap.
759 *Econometric Reviews* 23, 53–70.

- 760 Rockafellar, R. T. and S. Uryasev (2000). Optimization of conditional value-at-risk. *Journal of*
761 *Risk* 2, 21–42.
- 762 Spurgon, R. B. (2001). How to game your Sharpe ratio. *Journal of Alternative Investments* 4:3
763 (*Winter*), 38–36.
- 764 Strub, M., D. Li, and X. Cui (2019). An enhanced mean-variance framework for robo-advising
765 applications. SSRN 3302111.
- 766 Ungar, J. and M. T. Moran (2009). The cash-secured putwrite strategy and performance of related
767 benchmark indexes. *Journal of Alternative Investments* 11:4 (*Spring*), 43–56.
- 768 van Staden, P. M., D.-M. Dang, and P. Forsyth (2018). Time-consistent mean-variance portfolio
769 optimization: a numerical impulse control approach. *Insurance: Mathematics and Economics* 83,
770 9–28.
- 771 van Staden, P. M., D.-M. Dang, and P. A. Forsyth (2021). On the distribution of terminal wealth
772 under dynamic mean-variance optimal investment strategies. *SIAM Journal on Financial Math-*
773 *ematics* 12, 566–601.
- 774 Vigna, E. (2014). On efficiency of mean-variance based portfolio selection in defined contribution
775 pension schemes. *Quantitative Finance* 14, 237–258.
- 776 Vigna, E. (2022). Tail optimality and preferences consistency for intertemporal optimization prob-
777 lems. *SIAM Journal on Financial Mathematics* 13:1, 295–320.
- 778 Wang, J. and P. A. Forsyth (2010). Numerical solution of the Hamilton-Jacobi-Bellman formu-
779 lation for continuous time mean variance asset allocation. *Journal of Economic Dynamics and*
780 *Control* 34, 207–230.
- 781 Zhou, X. Y. and D. Li (2000). Continuous-time mean-variance portfolio selection: a stochastic LQ
782 framework. *Applied Mathematics and Optimization* 42, 19–33.